RADIOCARBON, Vol 49, Nr 1, 2007, p 1–46

REPORT ON THE FIRST STAGE OF THE IRON AGE DATING PROJECT IN ISRAEL: SUPPORTING A LOW CHRONOLOGY

Ilan Sharon[1] • Ayelet Gilboa[2] • A J Timothy Jull[3] • Elisabetta Boaretto[4]

ABSTRACT. The traditional chronology of ancient Israel in the 11th–9th centuries BCE was constructed mainly by correlating archaeological phenomena with biblical narratives and with Bible-derived chronology. The chronology of Cyprus and Greece, and hence of points further west, are in turn based on that of the Levant. Thus, a newly proposed chronology, about 75–100 yr lower than the conventional one, bears crucial implications not only for biblical history and historiography but also for cultural processes around the Mediterranean. A comprehensive radiocarbon program was initiated to try and resolve this dilemma. It involves several hundreds of measurements from 21 sites in Israel. Creating the extensive databases necessary for the resolution of tight chronological problems typical of historical periods involves issues of quality control, statistical treatment, modeling, and robustness analysis. The results of the first phase of the dating program favor the new, lower chronology.

INTRODUCTION

The construction of an "Old World chronology" of the Bronze and Iron ages (4th–1st millennia BCE) was one of the major intellectual achievements of the late 19th–early 20th centuries. However, it was a complicated web, spun out of snippets of contemporary information, inlaid in a mesh of later-written (hi)stories of varying credibility and agenda. It was synchronized by linking archaeological finds and phenomena across different, often faraway regions, and pegged to an absolute time scale by a few ancient astronomical observations, the understanding of which is in dispute (cf. Ward 1992). Recent years have seen crushing critiques of these, some even of the web in its entirety (e.g. James et al. 1992). There is an increasing call to bolster this chronology, if not altogether replace it, with scientifically derived chronometry, namely ^{14}C and dendrochronology (Renfrew 1991).

Several major projects launched in the last decade aim to do just that—at different geographical areas and historical periods. Some Old World examples are The Aegean Dendrochronology Project (www.arts.cornell.edu/dendro/); dating the Early Bronze Age in the Ancient Near East (the ARCANE project; www.arcane.uni-tuebingen.de); 2nd millennium chronology around the Mediterranean (the SCIEM project, see www.sciem2000.info/Pr05main.html); the date of the Thera eruption and its repercussions (e.g. Manning et al. 2006 with further bibliography there); dating the end of the Late Bronze Age (e.g. Manning et al. 2001); the Italian Iron Age (Nijboer et al. 2001); and dating the Phoenician and Greek colonization of the western Mediterranean (e.g. Torres Ortiz 1998; Botto 2004; Mederos Martín 2005).

Indeed, trying to resolve the chronological sequence of social, economic, and political processes that interest historians and archaeologists of historical periods is a challenge for the radiocarbon method, as they require much higher resolution than do *longue durée* processes typically studied by prehistorians and geologists. Working so close to the limit of precision of the analytic technique requires first of all very large data sets and also the development of rigorous protocols for quality control—in the field and in the laboratory—and of the statistical treatment of the results. Such measures, should they prove effective, could open new horizons for the collaboration between archaeologists, historians, and physicists.

[1]Institute of Archaeology, Hebrew University, Jerusalem, Israel. Corresponding author. Email: Sharon@mscc.huji.ac.il.
[2]Zinman Institute of Archaeology, University of Haifa, Israel.
[3]NSF-Arizona AMS Facility, University of Arizona, Tucson, Arizona.
[4]Radiocarbon Dating and Cosmogenic Isotopes Laboratory, Weizmann Institute of Science, Rehovot, Israel.

THE ARCHAEOLOGICAL/HISTORICAL PROBLEM

In the late 13th/early 12th centuries BCE, the Late Bronze Age sociopolitical systems in the Aegean and the eastern Mediterranean collapsed (e.g. Ward et al. 1992). The disappearance of these administrations means an almost total lack of contemporary written sources and of epigraphic finds in clear archaeological associations, which renders impossible direct historical dating of the following centuries (12th–9th centuries BCE).

Ancient Israel was until recently considered an exception. The deeds of its kings were recorded in the Bible, and dated by biblical king lists. Archaeologists associated constructions and destructions in the relevant sites with the biblical record and thus obtained dates for pottery assemblages associated with these "events." Comparative cross-dating with such "biblical" strata is a major peg upon which the early Iron Age chronology of the Levant, Cyprus, Greece, and even regions farther afield is largely dependent (see summary and references in Gilboa and Sharon 2003:64–72). Any shift in the former would entail re-adjustments of all these chronological constructions, and dictate rethinking of nearly every early Iron Age cultural process in these regions (e.g. Fantalkin 2001; Gilboa and Sharon 2001, 2003; Kopcke 2002; Coldstream 2003; Mederos Martín 2005).

However, in Israel too, pegs of absolute chronology are nonexistent for these centuries. Archaeologically, the Iron Age in Israel/Palestine is roughly divided into 2 segments, based mainly on the occupational sequence in the Central Hill country: "Iron I," in which the highlands were apparently settled by egalitarian rural societies; and "Iron II," which displays in this region phenomena customarily equated with a state system (settlement hierarchy, fortified administrative centers, and the like). Turning to the historical scenario *as portrayed in the Bible*, especially the "Deuteronomistic History" (the books of Deuteronomy through Kings; cf. for example, Knoppers and McConville 2000), it was only natural to associate "Iron I" with the tribal society described in Joshua–Judges, and to start "Iron II" with the United Monarchy of David and Solomon. Using the biblical king lists and "dead reckoning" from Assyrian, Babylonian, and Persian synchronisms at the end of the Iron Age, the Iron Age I|II transition—the beginning of David's reign—should fall somewhat before 1000 BCE. More specifically, the terminus ante quem for the "Iron I" | "Iron II" transition is customarily placed at 980 BCE (e.g. Mazar 1990: chapter 8). This was based on the assumption that the destructions typifying late Iron I sites were caused by this monarch's conquests, and that subsequent reconstruction should be attributed to the building projects of Solomon. The expansion of David's kingdom started, according to biblical narratives, before his 7th year and concluded well before the end of his 40-yr reign (about 970 BCE), when he is portrayed as ailing, elderly, and contending with civil unrest and palace intrigue.

Since the 1970s, the historical validity of the relevant biblical narratives has increasingly been questioned, contending, *inter alia*, that the Israelite "United Monarchy" is a socially/politically motivated construct of much later periods (e.g. Thompson 1999; and see summary and critique in Dever 2001:23–52). The controversy spilled over into archaeology when it was suggested that the Iron Age I|II transition be lowered from about 1000/980 to 925/920 BCE (Finkelstein 1996). This means that Iron Age IIA phenomena conventionally associated with David's and Solomon's United Monarchy post-date the reign of these kings by biblical reckoning. The 10th century, assigned by this chronology to the Iron Age I archaeological horizon, thus lacks clear material remains befitting an organized state, much less the Davidic/Solomonic empire described in the Bible.

The contention that the biblical portrayal of David's vast conquests and Solomon's wealth and power cannot be demonstrated archaeologically fed into a long-standing dispute in biblical studies between so-called "maximalists," scholars contending that the biblical narratives should be taken at

face value unless manifestly contradicted by outside evidence, and "minimalists," whose basic stance is that no biblical text can be taken literally unless corroborated by an outside source. This generated a fierce debate, which soon captured popular interest and even acquired political and religious overtones (summarized in Dever 2001). Lacking an answer to the chronological dilemma, dramatically different histories of ancient Israel are being written (e.g. Dever 2001 vs. Finkelstein and Silberman 2001, 2006; for recent summaries of the debate, see Finkelstein 2005; Mazar 2005).

PREVIOUS RESEARCH

Until the mid-1990s, the use of ^{14}C dating for the Iron Age in the Levant (and elsewhere) has been sporadic. Since then, 2 major excavation projects in Israel produced extensive *sequences* of early Iron Age ^{14}C determinations.

The first to produce a substantive set of pertinent dates was the coastal site of Tel Dor. Twenty-two samples, mostly charcoal, measured by liquid scintillation decay counting (LSC) at the Radiocarbon Dating Laboratory, Weizmann Institute of Science in Rehovot, supported the Low Chronology, placing the Iron Age I|II transition in the early 9th century BCE (Sharon 2001; Gilboa and Sharon 2001; 2003). This "ultra low" data set was the first empirical demonstration that the Low Chronology cannot be brushed off.

Adherents of the High Chronology claimed that the Dor results were "ambiguous" and inconsistent, that the stratigraphy at Dor is "complicated," the periodization too detailed (Bruins et al. 2003:316; Coldstream and Mazar 2003: n.14; Mazar 2004:33–34; Mazar 2005: n.6), and therefore the entire typostratigraphic and chronological seriation scheme at Dor is erroneous. A detailed elucidation of the stratigraphy, pottery typology, and chronological scheme used at Dor and its chronological correlation to other regions in Israel and overseas was produced by Gilboa and Sharon (2003; cf. also Gilboa 1999a,b), and some further comments will be made below.

Criticism of the first Dor data set also included the allegation that the results produced at the Rehovot laboratory in the 1990s were biased (Mazar 2004:24; Mazar et al. 2005:252–253). To address the question of bias, we conducted, in the framework of the current program, an intercomparison exercise between the major laboratories involved: the Radiocarbon Dating and Cosmogenic Isotopes Laboratory, Weizmann Institute of Science in Rehovot (henceforward Rehovot); the NSF Arizona AMS Laboratory, University of Arizona, Tucson (henceforward, Tucson); and (to a more limited extent) the Center for Isotope Research at Groningen (henceforward Groningen). This comparison showed no systematic difference among the laboratories (Boaretto et al. 2005).

In addition, 9 more samples, from the same stratigraphical sequence at Dor that produced the 1990s dates, were measured in 2004/2005 at Rehovot and Tucson (Table 7: 4522, 4525, 4528, 4531, 4532, 4540, 4541, 4542, 4556), two of which were also dated at Groningen (Table 7: 4531, 4540). All were analyzed by accelerator mass spectrometry (AMS). This new Dor data set produces a slightly higher (though not significantly so) Iron Age I|II transition, about 900 BCE, which still unequivocally supports the Low Chronology and rejects the High one (Sharon et al. 2005:78–82). This corroborates our previous conclusions, which were based on the 1990s set.

Shortly afterwards, however, a second sequence consisting of 34 dates from the site of Tel Rehov in the Jordan valley was published, measured with gas proportional decay counting (GPC) and AMS at Groningen (Bruins et al. 2003). It was claimed by the Rehov investigators to prove an "amended high chronology." Maximalists were quick to embrace this data set as "the last nail in the coffin of the 'low chronology'" (quotations from Holden 2003:229), while generally ignoring or belittling the contrary evidence.

https://doi.org/10.1017/S0033822200041886 Published online by Cambridge University Press

In reality, the Rehov "amended high" chronology goes a long way towards the contentions of the Low Chronology. The "amended high" chronology starts the Iron IIA at 980 BCE (the lowest possible date still compatible with biblical reckoning) but stretches it until about 830 BCE, contra the conventional view of ending it at 925 BCE (e.g. Bruins et al. 2003:318; Mazar 2004:30–31). Both the Dor and Rehov data sets corroborate that the Iron IIA horizon incorporates the 9th century BCE. The debate thus centers on the 10th century alone, or in other words, on the placement of the Iron I|II transition—at about 980 or about 900?

Critics of the Rehov data set claimed that the statistical procedures used in the original publication were flawed (Finkelstein and Piasetzky 2003; Sharon et al., forthcoming) and that the investigators ignored other dates from Tel Rehov, which were manifestly different. In response, the Rehov team also produced an augmented data set and an improved model supporting their view (Bruins et al. 2005; Mazar et al. 2005).

Can the Tel Rehov and Tel Dor dates be reconciled? It does need to be pointed out that Tel Rehov (as excavated to date) overrepresents Iron IIA. Detailed Iron IIA sequences in several excavation areas in this site produced abundant ceramic assemblages and organic remains, while Iron Age I strata are only exposed in a narrow step-trench on the slope. At Dor, the situation is reversed. Five horizons of superimposed Iron I (and I|II transition) were excavated in several different areas, while Iron IIA is underrepresented. This can go part way towards explaining the apparent contradiction in the dating of these 2 sites.

Another consideration concerns the shape of the calibration curve in the relevant region (Figure 1). A random sample of dates in the 10th century should produce measurements in the range ~2850 to ~2750 BP, or even somewhat wider, allowing for analytical error. Dates in the 9th century should fall between 2770 (or even higher) and 2600 BP. The Groningen Tel Rehov measurements are in fact much more limited (~2800 to 2750 BP), giving the impression that the true chronological range of the Iron Age IIA phases at this site is the second half of the 10th century BCE and/or the first half of the 9th, rather than the first half of the 10th century as claimed.

The model chosen by the Rehov investigators allows for "gaps" between "destructions" and concentrates the dates into "events." This provides a neat explanation for the lack of dates in the 2850–2800 BP range, which one would otherwise expect. The combined effects of the shape of the curve at this particular region—the "gappy" model and the fact that late Iron I is poorly represented—conspire to push the beginning of the Iron II sequence at Rehov (stratum VI) onto the little downwards wiggle at about 975–950 BCE, which is not necessarily warranted by the measurements alone.

Moreover, while the model presented by the Rehov team does posit a high probability (68%) that the boundary between phase D3 (late Iron I) and stratum VI (lowest Iron IIA) falls in the first half of the 10th century (990–960 BCE) there is a subsidiary peak to the distribution (Bruins et al. 2005:283), which indicates a significant possibility (about 20%) that it falls in the second half of the century (950–920 BCE). As noted above, the addition of Tel Rehov dates measured in laboratories other than Groningen enhances this peak (and in some models reverses the odds; see Sharon et al., forthcoming; cf. also Bronk Ramsey 2005:63).

This scenario perfectly exemplifies the danger of predicating the chronological scheme of an entire region on (one excavator's interpretation of) a single site or a limited set of samples analyzed by a single lab. A comprehensive study to resolve this problem was clearly in order.

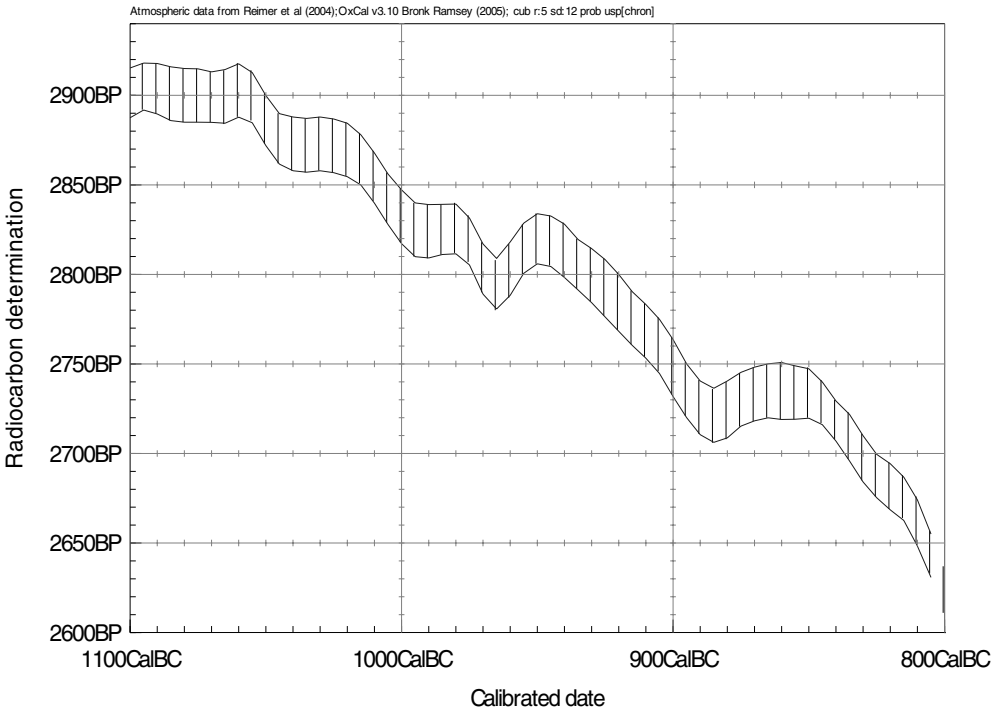

Figure 1 The IntCal04 calibration curve (Reimer et al. 2004) in the early Iron Age

THE CURRENT STUDY

To overcome these and other archaeological and analytical pitfalls in the dating process, the present project draws upon a wide range of dates from nearly all relevant sites in Israel. With generous grants from the Israel Science Foundation, we approached all the excavators of Iron Age I and IIA sites in the country and obtained (to date) 105 samples from 21 sites (Figure 2). These were replicated (see below) to produce 380 ^{14}C determinations, by far the largest data set bearing on the problem.

Choice of Samples and Archaeological Pitfalls

Quality control on sample collection in the field dictated that only samples originating in reliable contexts be used. Accordingly, together with the excavators, we attempted to obtain samples of either primary deposits, or otherwise uncontaminated fills, whose stratigraphic attributions are secure and with clear association to meaningful ceramic assemblages. Samples were selected from within such contexts based on size, state of preservation, and type of raw material—the preferred ones being short-lived samples (grain or olive pits). Despite all vigilance, some archaeological "noise" is inevitable; some cautionary tales are listed below.

Charcoal was only used if critical contexts or sites could not produce short-lived samples. In retrospect, charcoal indeed often produced dates that are obviously too old. One case in point: Five charcoal samples from strata XII/XI at Hazor (assays 3700–3704 in Table 7) were recovered from refuse pits with well-defined Iron Age ceramics, cut into the destruction debris of the Late Bronze Age palace. In some of these (3703, 3704), the date is hundreds of years too old (Middle Bronze Age, before 1600 BCE).[1] This indicates either reuse of constructional wood from the defunct palace, or redepo-

[1]All dates referred to herein as BCE are calibrated using the 2004 calibration curve (Reimer et. al. 2004). Uncalibrated dates are referred to as BP.

https://doi.org/10.1017/S0033822200041886 Published online by Cambridge University Press

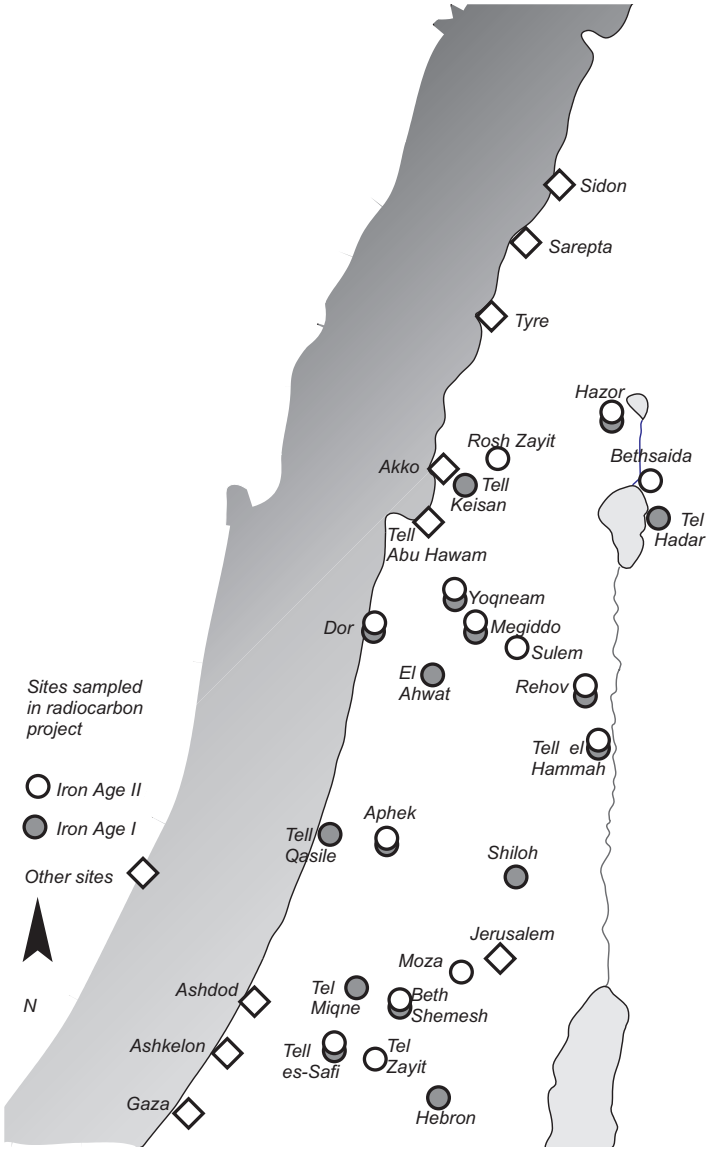

Figure 2 Map of date-producing sites

sition of charcoal from the palace destruction debris in later pits. The 3 other dates are equivocal. Our own database and other studies (Manning et al. 2001) show that dates in the range of 2950–3000 BP (about 1300–1100 BCE) may be encountered in both Late Bronze Age and early Iron Age contexts. Is this charcoal also redeposited, or can we regard these samples as bona fide?

Another type of problem was encountered at the site of Moza. Four samples (of charcoal) were taken from a "burnt layer" (L2043, samples 4583–4587 in Table 7). Above that burnt layer was a well-defined stratum of Iron II, but, on examination of the pottery from the burnt layer itself and from the fill above it, it turned out that the contexts included, in addition to some Iron Age pottery, redeposited potsherds of earlier periods (Bronze Age). Can this charcoal be used to date the Iron IIA?

https://doi.org/10.1017/S0033822200041886 Published online by Cambridge University Press

Nor is the use of only short-lived materials foolproof. A case in point is sample 4278 from Tel Zayit, which gave a date more than a thousand years too young (in the Middle Ages). The sample came from a pit, some 50 cm below topsoil. The pottery from the pit was entirely Iron Age. Possible explanations are an unnoticed intrusion (e.g. a rodent burrow) or that the pit was indeed dug in the Middle Ages (a period attested at this site), but no contemporary pottery was deposited in it for one reason or another. When the date is a thousand years too young (and has been verified, as in this case, by replication), the problem is clearly archaeological (an intrusion). But how many other intrusions exist where the difference is only a few decades (e.g. an undetected intrusion from one stratigraphic phase to the one immediately preceding it)?

In a few other cases, excavators changed their minds about the attribution of contexts that were sampled. In one case (e.g. sample 4288 from Tel Miqne), ^{14}C analysis indicated a much later date than the relative archaeological context supplied by the excavators. In a re-examination of the context, it was recognized that the locus was contaminated by intrusive material. In another case from the same site (sample 4282), the excavators changed the phase designation without any indication from the ^{14}C dates that something was amiss (note the different stratigraphic designation in Table 7 vs. Boaretto et al. 2005: Table 1).

As a last case in point: Sample 4281 is from a granary under the stratum V gate at Bethsaida, and hence is attributed by the excavator to stratum VI. The context itself did not yield any indicative pottery. The excavator dates stratum VI to Iron IIA, but this dating is based on an assemblage found in another excavation area, some 30 m away. The quality of the organics (many liters of burnt grain) however, was such that we felt we had to sample it, pending substantiation of the claim that it dates to the Iron Age IIA.

Such cases serve as reminders that the link between the ^{14}C sample and the cultural episode one wants to date is never straightforward, and as warnings that in any database, other, less evident, archaeological errors may exist. The opposing danger is that in not reporting on suspect samples, one may unwittingly be biasing the database in favor of one's preconceived notions (naturally a date in keeping with one's belief would not be suspect). We adopted a strategy of transparency: we tried to discriminate in our choice of samples, but once a sample has been chosen and dated it is not removed from the database.

^{14}C ANALYSIS AND QUALITY CONTROL IN THE LABORATORIES

^{14}C analysis was performed mainly in the Rehovot and Tucson laboratories, using both LSC and AMS techniques, and several samples were also dated at Groningen, using AMS. Quality control in the laboratories consisted of the following procedures: AMS was chosen as the primary method for this study, as size constraints prevent decay counting to be replicated except for exceptionally large samples. In 14 of these larger samples, the bulk of the sample was turned to benzene for liquid scintillation counting (usually only a single vial could be extracted, denoted in Table 7 as "Rehovot LSC"), but some was set aside for graphitization for AMS. AMS was always performed on multiple targets (except for a few cases that were too small or in which one or more of the targets was a dud). Specimens of all the samples labeled "Rehovot AMS" were pretreated as described in Alon et al. (2002; Yizhaq et al. 2005), graphitized in Rehovot, and then run in Tucson. Twenty-two samples were split between the 2 laboratories before cleaning (Boaretto et al. 2005). In these cases, charcoal samples were mechanically cleaned and homogenized prior to splitting, while olive seeds were sent raw and complete. One portion was then pretreated at Rehovot (as described above) while the other portion (measurements listed in Table 7 as "Tucson AMS") was both pretreated and measured at Tucson.

Intercomparison was also conducted with the Groningen Center for Isotope Research, on 8 samples. These include 5 samples split between Rehovot and Groningen (3778, 3931, 4410, 4531, 4540), according to the same protocol as above (see also Boaretto et al. 2005). Sample 3778 was also part of the Rehovot–Tucson intercomparison exercise and also dated by LSC. Three additional samples (3805, 3807, 3809) were from contexts at Tel Rehov previously examined at Groningen and reported in Bruins et al. (2003). In these 3 cases, the samples we dated were from the same *contexts* but are not necessarily identical. All 3 were dated at Groningen by GPC and one also by AMS. One of them (3807) was also dated (twice) by LSC in Rehovot, and another (3809) by AMS in Tucson.

In cases that showed anomalies, a second run of AMS was performed. On average, each sample was measured 3 times, but some were measured as many as 9 times. In a few cases, where anomalies were linked to specific experimental protocols or laboratory procedures (see details in Boaretto et al. 2005; Sharon et al. 2005), the entire set of measurements performed under such conditions was excluded—whether or not the results were divergent. In no case, however, was a measurement summarily dismissed simply because "it does not fit." A case in point: in sample 3943, the third cathode produced an age more than 3 standard deviations away from the average. The reason for this may have been graphite improperly pressed into the cathode, as has been the case in some other anomalous measurements (Boaretto et al. 2005; Sharon et al. 2005). However, in this case the cathode was not available for inspection and therefore this measurement was not removed from the list.

OUTLIER ANALYSIS

The extensive replication procedure also allows for a rigorous treatment of outliers. The different options we considered for identifying and treating aberrant results are discussed in detail in Boaretto et al. (2005:43) and Sharon et al. (2005:71–78). In this paper, we only present briefly the results as they pertain to the database presented here. First, we calculated the weighted average of each replicated set and computed the standardized residual (Scott 2003:383; Sharon et al. 2005:72) for each measurement. An overall χ^2 statistic was defined as the sum-of-square-residuals over the entire database, and the highest absolute residuals were excluded from the data set in a stepwise fashion, until the overall significance (α) of the overall χ^2 dropped below 5%. Out of 380 measurements, this state ($\alpha = 10\%$) was reached after the removal of the 4 highest residuals (1% of the total).

We give here 1 example to illustrate the process and its potential problems. Sample 3932 (legumes from the late Iron I destruction of stratum X at Tell Qasile) produced the following results (see Table 1).

Of the 6 measurements, one is very low (3932.6) and one is very high (3932aa), and indeed the χ^2 (for this assay only) is rather high, giving less that 1% probability of this spread being entirely random. Removing 3932.6 would give a weighted date of 2779 ± 20 BP and a χ^2 value of 8.34 (α = 8%), while removing 3932aa would produce a weighted average of 2724 ± 20 BP and a χ^2 of 7.07 ($\alpha = 13\%$). In each case, the truncated data set would have passed the χ^2 test. Note, however, that the standardized residual of 3932aa is the highest in the set (in absolute value) and that, indeed, removing 3932aa results in a better overall fit for the rest of the measurements. Thus, our procedure would prefer to remove this measurement. As assay 3932 is indeed one of the very low dates in Iron I, the 50-yr difference between the 2 averages may actually be significant for the overall result. However, this is indeed the extreme case. In most other assays, the outlying measurement was unambiguous.

This, however, is not the end of the story. While having 2 measurements out of 6 vary by more than 2 standardized residuals from the norm is indeed highly unlikely, in a study involving over 350 mea-

Table 1 Six replications of sample 3932. Potential outliers are in bold.

Site & stratum	Type	Sample	Analysis	Age (BP)	σ	W. AVG	C σ	Residual	χ^2	df	σ	Relative date
Qasile X L168	Lathyrus	3932.3	Rehovot AMS	2745	50	2752	18	–0.1437	16.6	5	1%	Iron I (l)
		3932.4	Rehovot AMS	2765	75			0.17084				
		3932.5	Rehovot AMS	2685	50			–1.3437				
		3932.6	Rehovot AMS	**2650**	40			**–2.5547**				
		3932a	Tucson AMS	2780	35			0.79467				
		3932aa	Tucson AMS	**2862**	40			**2.74533**				

surements we should expect to find several deviations of such magnitude. Indeed, the stepwise removal of outliers has reached an acceptable level of agreement before any of the sample 3932 measurements had been removed. In this case, the prudent course was to leave both measurements in.

After removal of outliers in this fashion, weighted averages were recalculated per sample, and the measurement errors combined to produce reduced error estimates. These are referred to below as "combined dates."

Concurrently, we used another procedure. Along with the weighted average and combined error estimates we also calculated—before removal of any suspected outliers—the (unweighted) average for each sample and the standard deviation between the measurements. Of the 2 pairs of central moments and error estimates, we then used the one with the larger deviation (Bevington and Robinson 1992). We refer to this method below as "cautious error estimation." There is some indication that conventional error-estimation techniques may tend to underestimate the actual deviation that would be obtained under extended replication (Scott et al. 2003:213–218, 252–260, and Figures 7.1–7.7). This method, on the contrary, almost certainly overestimates them. In the case of assay 3932 (see Table 1), the "cautious" estimate of the date would be 2748 ± 68 BP.

A third way of treating analytic outliers (or, rather, of not treating them) is to simply not combine the measurements, and model the archaeological phases with the individual measurements as point estimates, rather than with a single estimate per sample. This would essentially move the onus of identifying outliers to the next stage of analysis. The logic behind this would be: "If we don't know if measurement X or Y is [more] correct, let's put them both in the model and see how they fit with other measurements of the same archaeological horizon." Such a procedure is open to objection on 2 grounds. First, it tends to give extra weight to samples that were replicated many times. Note, however, the fact that combining measurements always reduces the error estimate (regardless of how similar or dissimilar the actual measurements are!) and causes the exact same effect. Secondly, several replicated measurements of the same sample cannot be regarded as statistically independent. The question of dependence is complex, and is most often ignored in archaeological studies. Can several (different) samples from the same locus or layer in a site be considered independent? Often, we do not even know if they represent the same event or not. An even more complex question, in a study like ours that considers different sites, is the effect of a regional sequence that is out of synch (even slightly so) with another one. In such a case, we might be consistently sampling something

https://doi.org/10.1017/S0033822200041886 Published online by Cambridge University Press

slightly earlier, or slightly later, in one site or region than in another. We may, however, at least assert that given that the horizons being sampled are fairly short (relative to the analytical error), fairly (though not perfectly) well-defined, and fairly densely sampled, the effect of these complex dependencies and partial dependencies would be quite small. At any rate, we regard "uncombined" models as suspect, though they are included here for the purpose of robustness analysis.

RELATIVE PERIODIZATION OF THE IRON AGE I–IIA IN ISRAEL

The date-producing contexts were seriated by intersite stratigraphical order and intrasite ceramic considerations and clustered into 8 chronological horizons. The basis for this subdivision was extensively discussed in Gilboa and Sharon (2003) and Sharon et al. (2005). We offer here some justification of the scheme as a whole, without going into minutiae of specific pottery types or why a particular stratum was classified to horizon X and not X+1.

A typochronological framework was first devised for the Phoenician coast (including Dor), which is the region that offers the most detailed early Iron Age stratigraphic/ceramic sequences in the southern Levant. It also allows a high-resolution tracing of typological developments of vessels/wares that are also frequently found outside this region and thus can be used to overcome problems of ceramic regionalism. The most important among them are painted Cypriot, Phoenician, and Philistine ceramics. Though we devised a new chronological terminology for Phoenicia (Gilboa and Sharon 2003:10–11), the basic typological criteria with which we attempted the subdivision of the Iron Age I are well known and widely accepted in the archaeological community.

The painted pottery typical of Philistia undergoes a sequence of stylistic development: The initial finely-levigated and highly-fired Monochrome ware with Aegean forms and freehand designs (Dothan and Zukerman 2004) is replaced by "Philistine Bichrome" (Dothan 1982: chapter 3), which gradually "degenerates" (e.g. Dothan 1982:191–198); "Canaanizes" (Mazar 1985:119–120); "acculturates" (Stone 1995:19); "Creolizes" (Maeir 2004). In other words, it loses its distinctively Aegean form and decoration, is often red-slipped, and the painted decoration often becomes simple and schematic. Finally, it transforms into the "Late Philistine Decorated Ware" typical of the Iron Age IIA (Ben-Shlomo et al. 2004), in which the geometric decoration (black and white on red slip) is instrumentally applied.

In Phoenicia, meanwhile, "late Canaanite ware" or "Phoenician monochrome" (Gilboa 1999a) transforms into the famed "Phoenician Bichrome," which is typical of the later part of Iron I and goes on (with several distinct changes) into Iron II (Anderson 1990; Gilboa 1999a), when it begins to appear together with "Phoenician Red Slip."

These 2 trajectories are corroborated by the evolution of Cypriot ceramics: The end of the "real" Late Bronze Age (LB) in the Levant parallels the Late Cypriot (LC) II. Typical LC II imports, such as White Slip and Base Ring wares, which are found in abundance in all LB sites, cease towards the very end of the Levantine Bronze Age. Then comes LC IIIA, which by Cypriot imports in the Levant, and vice versa, correlates with the horizon here termed the LB|IR transition (for which see below) (e.g. D'Agata et al. 2005). LC IIIB imports have not been found in Israel, but the following Cypro-Geometric (CG) IA is found in the same contexts with the earliest Phoenician Bichrome both in Cyprus and in Phoenicia (Iacovou 1999; Gilboa 1999b; Gilboa and Sharon 2003). This evolves, via the CG IB–CG II stage (e.g. Coldstream 1999; Sharon et al. 2005:68–70 and references) to CG III, mostly represented by Cypriot Black on Red ware. The latter is evident in almost all Iron IIA assemblages in the Levant (Schreiber 2003: mainly chapters 3 and 4; Gilboa and Sharon 2003:62–63, 66–67).

Table 2 Samples seriated into 8 chronological horizons. LB = Late Bronze Age; IR = Iron Age. The italicized numbers are the sample numbers. Asterisks denote charcoal samples (the rest are short-lived samples). The individual measurements for each sample are listed in Table 7.

LB	LB|IR	IR I		IR I|II	IR IIA		IR IIB
Aphek X12: *4510* **Tel Zayit:** *4274*	**Megiddo K/6 [=VIIA?]:** *4499, 4500, 4501* **Miqne VIIb:** *4286* **Keisan 13**: *3804**	**Ahwat:** *4270, 4271, 4272, 4273* **Hazor XII/XI:** *3700*, 3701*, 3702, 3703*, 3704** **Shiloh V:** *3927, 3928, 3929* **Hebron VII:** *4147*, 4148** **Rehov D4:** *3809*		**Dor D2/ 8c:** *4540, 4541, 4542* **Aphek X8:** *4511*	**Rosh Zayit IIA:** *3797, 3798, 3799* **Rehov D/2:** *3807* **Rehov E/1b**: *3808* **Bethsaida *6*:** *4281* **Sulem:** *3989*, 3990*, 3991** **Moza**: *4583*, 4584*, 4586*, 4587**		**Beth Shemesh 3:** *3937, 3938* **Tel Zayit I:** *4275, 4278, 4279*, 4280**
		IR I (e)	IR I (l)		IR IIA	IR II A|B	
		Beth Shemesh 6: *3934* **Beth Shemesh 5:** *3935, 3936* **Dor D2/ 13:** *4528* **Dor D2/ 12:** *4522, 4525* **Miqne VIb**: *4283* **Miqne Vb:** *4282, 4284*	**Megiddo K-4 =VIA:** *3939, 3940, 3942, 3943, 3944, 3945, 3946* **Qasile X:** *3853, 3930, 3931, 3932, 3933* **Dor D2/10-9:** *4531, 4532* **Tel Hadar IV:** *3795, 4291* **Rehov D3:** *3805, 3806* **Hammah [lower]:** *4416*, 4417* **Keisan 9b:** *3801** **Keisan 9a-b:** *3802** **Keisan 9a:** *3796, 3803** **Yoqne'am XVII:** *3777, 3778, 3779**		**Hazor X:** *3782*, 3783*, 3784, 3786* **Megiddo H5 [=IVB-VA]:** *3949* **Yoqne'am XIV**: *3780** **Hammah [mid]:** *4411, 4412, 4413, 4414, 4415, 4418, 4419, 4420, 4423, 4424, 4425* **Dor D2/8b:** *4556*	**Safi IV:** *4409, 4410* **Hammah [upper]:** *4422* **Hazor IX:** *3785**	
Total: 2	**Total: 5**	**Total: 9**	**Total: 27**	**Total: 4**	**Total: 18**	**Total: 4**	**Total: 6**
		Total: 51			**Total: 35**		
Grand total (samples): 103							

In order to avoid the debate as to whether sites with finds relating to the Egyptian 20th Dynasty should be relegated to the end of the Late Bronze Age or to "Iron Age IA" (Ussishkin 1985 vs. Mazar 1990:290), and whether they pre-date or coincide with the first appearance of Philistine wares (the latter possibility, however, is our preference; see summary of the different views in Finkelstein 2000:162–165), we grouped these together into a category we label, for convenience, "LB|IR transition." "Terminal Late Bronze Age" assemblages that no longer have Cypriot/Mycenaean imports, assemblages with 20th Dynasty Egyptian artifacts, or "Philistine Monochrome" and/or LC IIIA imports were all placed under this label.

Assemblages with "Philistine Bichrome" and/or pre-dating the appearance of "Phoenician Bichrome" were classified as "Iron Age I (early)," while those exhibiting the late "degenerate" phase of Philistine decoration and/or Phoenician monochrome, early "Phoenician Bichrome," and/or having CG IA imports were classified as "Iron Age I (late)."

https://doi.org/10.1017/S0033822200041886 Published online by Cambridge University Press

The transitional Iron I|II horizon is that postdating the late Iron I levels and preceding the "classical" Iron IIA occupations, and is coeval with Cypriot CG IB-II. The chronological significance of this horizon has been recognized lately by scholars dealing with northern sites in Israel (with some variations, e.g. calling it "early Iron IIA"). (For an explicit discussion of this horizon, see Sharon et al. 2005:67–70; Zarzecki-Peleg 2005:368, 376; cf. also Mazar 2004:68.) This horizon does not parallel "late Iron I" at Tel Rehov, as suggested in Mazar (2005: n. 6). If anything, it should correspond to stratum VI, in as much as this stratum precedes the beginning of CG III wares at Rehov.

There is a general agreement on occupational strata assigned to Iron IIA (see Mazar 2005: Table 24; for the pottery, Ben-Tor and Zarzecki-Peleg, forthcoming), but divisions *within* this period are difficult (that, in itself, might indicate that it is fairly short). In our terminology, Iron IIA strata in the north are the "classic" Iron IIA strata (considered Solomonic by the High Chronology). All of these strata contain Cypro-Geometric III pottery and some have Euboean Sub-Proto-Geometric imports too. Correlation with Iron IIA sites in the south is more complex. Regarding Judah, Herzog and Singer-Avitz (2004) suggested lately that the horizon hitherto regarded there as late Iron I be termed "early Iron IIA." This horizon probably corresponds to our transitional horizon, and their "later Iron IIA" probably parallels our Iron IIA. Because we do not possess samples from this region, we did not tackle this issue further. Occupations stratigraphically placed late in the Iron IIA sequences in their respective sites were termed Iron IIA|B (cf. Zarzecki-Peleg 2005:376). Some contexts were defined as "general Iron IIA," with no attempt at subdivision.

In as much as the scheme proposed herein has any novelty, it is in being explicitly seriative—every 2 temporal categories have an "intermediate" between them. We use the symbol | to denote this. This reflects our conviction that change in artifactual assemblages is gradual, quantitative, and durative, i.e. "types" do not appear or disappear overnight but rather slowly and constantly gain or lose popularity as well as undergo gradual morphological change. This, of course, is hardly revolutionary, and yet the very fact that the periodization models we use force us to pigeonhole assemblages in "periods" encourages a punctuative view of cultural change—in which one envisions instantaneous upheaval between periods vs. no change at all within the period itself (e.g. Mazar 2005:21).

The other feature that characterizes the proposed scheme is that it allows for the inclusion of assemblages that cannot be precisely placed, other than in a very general category ("Iron I" or "Iron IIA"). Some assemblages defy very precise seriation, either because of the nature of the assemblage, the nature of the site, the nature of the excavation, or the nature of the publication.

An important case in point: the "Israelite Settlement" sites in the hill country are poorly seriated. These are often single-occupation and/or very shallowly stratified sites, so building a typological sequence based on internal stratification is impossible. They are also usually very poor sites, so correlating them with richer (and more richly stratified) sites in the lowlands on the basis of imports is difficult. Very few of them are excavated, even fewer are adequately published, and many of these reports are rather old. The net result is that we are unable to offer a very precise seriation for a critical region for one of the central issues under debate (sites in the database in this category are Shiloh, Hebron, and El-Ahwat).

While the scheme as presented is indeed fairly complex, a complex scheme can always be simplified. In the following, we shall show several simplified models that were derived from this scheme. Indeed, the extent to which different (legitimate) models of the same data show similar overall results is a strong test for the robustness of the data set.

Having said all that, there still is, of course, an almost endless amount of tinkering that can be done with the models. Certainly, some archaeologists might feel that some assemblage that we are cautious about might be put in a more precisely seriated category, or vice versa. Some may suggest entirely different criteria to break the sequence of the same assemblages in different ways. Far be it from us to claim that the "Philistine potters' guild" decided to "degenerate" on the same day that the "Phoenicians" "invented" the Bichrome style. We only assert that such trajectories are useful tools for grouping together more-or-less contemporaneous assemblages. Indeed, this data set is so rich that it will probably serve as the basis for chronological modeling for years to come. Our purpose in the following is to present the data, together with what we think are the most reasonable ways to model it.

MODELING

The scheme introduced above allows for the main subject of interest—the transition between the Iron I and II—to be calculated using different Bayesian models, operating at different levels of resolution and employing different parts of the data. Each model was run both with all the relevant assays—short- and long-lived and on the short-lived assays only.

The simplest (and crudest) model is to lump together all the dates from Iron I contexts vs. all the dates for Iron II contexts (Table 3) and to model the likelihood of a boundary point in between these 2 groups. Below, this is referred to as "the coarse model." In OxCal (Bronk Ramsey 2001) notation, this simple model is presented in Figure 3.

This model does not include Late Bronze Age and transitional LB|IR contexts. It also does not include the contexts labeled "transitional Iron I|II." This might introduce a problem, as we a priori know that there is a gap between the 2 categories. One can try 2 additional models wherein these dates are either regarded as "late Iron I" or "early Iron II," and lumped with the appropriate group; but we have not done so in this instance. Samples excluded at the outset were the Tel Zayit Middle Ages one and the Hazor Middle Bronze Age ones. Though we explained above our reluctance to exclude samples from the data set, such huge misfits simply prevent the convergence of the algorithm; and the fact that these dates are out of the bounds of discussion is obvious. Other extremely high (and extremely low) dates (e.g. assay 3625 from Dor D2/12, which at 3029 ± 28 BP is definitely earlier than 1200 BCE) were initially left in (see below for treatment of misfits).

Another simple model that can be drawn from the data set will be referred to as the "focused model" (Figure 4). It uses only the most relevant contexts for the question at hand, i.e only those of the late Iron I, transitional Iron I|II, and early Iron IIA horizons. Of interest to us in this case are 2 boundaries: the one between late Iron I and the "transitional" horizon, and the one between the "transitional" horizon and the "classical" Iron IIA. The advantage of this model is that it disregards contexts that are far removed from the transition we are after, and imprecisely seriated ones, but it uses only 49 of the 109 assays. If we limit ourselves to short-lived samples, only 40 assays are used (Table 4).

Finally, the third model is the one representing the entire scheme utilizing as much information as possible. We call this the "composite model" (Table 5 and Figure 5). Within the basic sequence of 6 typological horizons, the Iron I and Iron IIA were further divided (by an *internal* sequence) into early and late sub-phases. This model allows us to use dates from "unordered" Iron I and Iron IIA contexts, as well as ones for which a finer attribution can be offered.

Table 3 The coarse model. Contexts and sample numbers (in italics) are listed, charcoal samples with asterisks. The shaded cells are ones not used in this model. Crossed-out samples are misfits excluded during the model run (see below). Totals in parentheses exclude charcoal samples.

LB	LB|IR	IR I		IR I|II	IR IIA		IR IIB
Aphek X12: *4510* Tel Zayit: *4274*	Megiddo K/6 [=VIIA?]: *4499, 4500, 4501* Tel Miqne VIIb: *4286* Keisan 13: *3804**	El Ahwat: *4270, 4271, 4272, 4273* Hazor XII/XI: 3700*, 3701*, 3702, ~~*3703**~~,~~*3704**~~ Shiloh V: 3927, *3928, 3929* Tel Hevron VII: *4147*, 4148** Tel Rehov D4: *3809*		Dor D2/8c: *4540, 4541, 4542* Aphek X8: *4511*	Rosh Zayit IIA: *3797, 3798, 3799* Rehov D2: *3807* Rehov E1b: *3808* Bethsaida *6: 4281* Sulem: *3989*, ~~*3990**~~, *3991** Moza: *4583**, ~~*4584**~~, *4586**, ~~*4587**~~		Beth Shemesh 3: *3937, 3938* Tel Zayit I: *4275*, ~~*4278*~~, *4279**, *4280**
		IR I(e)	IR I(l)		IR IIA	IR IIA|B	
		Beth Shemesh 6: *3934* Beth Shemesh 5: *3935, 3936* Dor D2/13: *4528* Dor D2/12: *4522, 4525,* Miqne VIb *4283* Miqne Vb *4284*	Megiddo K/4 =VIA: *3939, 3940, 3942, 3943, 3944, 3945, 3946* Qasile X: ~~*3853*~~, *3930, 3931,* ~~*3932*~~, *3933* Dor D2/9-10: *4531, 4532* Tel Hadar IV: *3795, 4291* Rehov D3: *3805,* ~~*3806*~~ Hammah [lower]: *4416*, 4417* Keisan 9b: *3801** Keisan 9a-b: *3802** Keisan 9a: *3796*, 3803** Yoqneam XVII: *3777, 3778, 3779**		Hazor X: *3782*, 3783*, 3784, 3786* Megiddo H/5 [=IVB-VA]: *3949* Yoqne'am XIV: *3780** Hammah [mid]: *4411, 4412, 4413, 4414, 4415, 4418, 4419, 4420, 4423, 4424, 4425* Dor D2/8b: *4556*	Safi IV: *4409, 4410* Hammah [upper]: *4422* Hazor IX: *3785**	
		Total: 49 (41)			**Total: 41 (28)**		

Total samples for model: 90 (69)

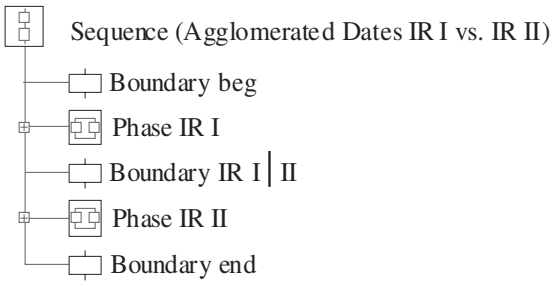

Figure 3 The coarse model: all Iron I dates vs. all Iron II dates

https://doi.org/10.1017/S0033822200041886 Published online by Cambridge University Press

Table 4 The focused model. Contexts and sample numbers (in italics) are listed, charcoal samples with asterisks. The shaded cells are ones not used in this model. Crossed-out samples are misfits excluded during the model run (see below). Totals in parentheses exclude charcoal samples.

LB	LB|IR	IR I		IR I|II	IR IIA		IR IIB
Aphek X12: *4510* Tel Zayit: *4274*	Megiddo K/6 [=VIIA?]: *4499, 4500, 4501* Miqne VIIb: *4286* Keisan 13: *3804**	El-Ahwat: *4270, 4271, 4272, 4273* Hazor XII/XI: *3700*, 3701*, 3702, 3703*, 3704** Shiloh V: 3927, *3928, 3929* Tel Hevron VII: *4147*, 4148** Tel Rehov D4: *3809*		Dor D2/8c: *4540, 4541, 4542* Aphek X8: ~~*4511*~~	Rosh Zayit IIA: *3797, 3798, 3799* Rehov D2: *3807* Rehov E1b: *3808* Bethsaida *6: 4281* Sulem: *3989*, 3990*, 3991** Moza: *4583*, 4584*, 4586*, 4587**		Beth Shemesh 3: *3937, 3938* Tel Zayit I: *4275, 4278, 4279*, 4280**
		IR I (e)	IR I (l)		IR IIA	IR II A|B	
		Beth Shemesh 6: *3934* Beth Shemesh 5: *3935, 3936* Dor D2/13: *4528* Dor D2/12: *4522, 4525,* Miqne VIb *4283* Miqne Vb *4282*, *4284*	Megiddo K/4 =VIA: *3939, 3940, 3942, 3943, 3944, 3945, 3946* Qasile X: *3853, 3930, 3931, 3932, 3933* Dor D2/9-10: *4531, 4532* Tel Hadar IV: *3795, 4291* Rehov D3: *3805, 3806* Hammah [lower]: *4416**, *4417* Keisan 9b: *3801** Keisan 9a-b: *3802** Keisan 9a: *3796*, *3803** Yoqne'am XVII: *3777, 3778, 3779**		Hazor X: *3782*, 3783*, 3784, 3786* Megiddo H/5 [=IVB-VA]: ~~*3949*~~ Yoqne'am XIV: *3780** Hammah [mid]: ~~*4411*~~, *4412, 4413, 4414, 4415, 4418, 4419, 4420, 4423, 4424, 4425* Dor D2/8b: *4556*	Safi IV: *4409, 4410* Hammah [upper]: *4422* Hazor IX: *3785**	
			Total: 27 (22)	**Total: 4**	**Total: 18 (15)**		
Total samples for model: 49 (41)							

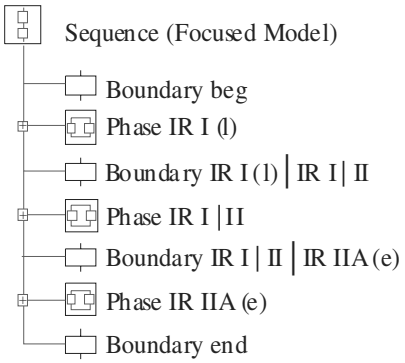

Figure 4 The focused model in OxCal notation

https://doi.org/10.1017/S0033822200041886 Published online by Cambridge University Press

Table 5 The composite model. Contexts and sample numbers (in italics) are listed, charcoal samples with asterisks. Crossed-out samples are misfits excluded during the model run (see below). Totals in parentheses exclude charcoal samples.

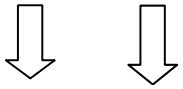

LB	LB|IR	IR I		IR I|II	IR IIA		IR IIB
Aphek X12: *4510* Tel Zayit: *4274*	Megiddo K/6 [=VIIA?]: ~~*4499*~~, *4500*, ~~*4501*~~ Miqne VIIb: *4286* Keisan 13: *3804**	El-Ahwat: *4270, 4271, 4272, 4273* Hazor XII/XI: *3700*, 3701*, 3702*, ~~*3703*~~*, ~~*3704*~~* Shiloh V: *3927*, *3928, 3929* Tel Hevron VII: *4147*, 4148** Tel Rehov D4: *3809* Total: 15 (9)		Dor D2/8c: *4540, 4541, 4542* Aphek X8: ~~*4511*~~	Rosh Zayit IIA: *3797, 3798, 3799* Rehov D2: ~~*3807*~~ Rehov E1b: *3808* Bethsaida *6:* ~~*4281*~~ Sulem: ~~*3989*~~*, ~~*3990*~~*, *3991** Moza: ~~*4583*~~*, ~~*4584*~~*, ~~*4586*~~*, ~~*4587*~~*		Beth Shemesh 3: *3937, 3938* Tel Zayit I: *4275*, ~~*4278*~~, ~~*4279*~~*, *4280**
		Total: 15 (9)			**Total 13 (6)**		
		IR I (e)	IR I (l)		IR IIA	IR II A|B	
		Beth Shemesh 6: *3934* Beth Shemesh 5: ~~*3935*~~, ~~*3936*~~ Dor D2/13: *4528* Dor D2/12: *4522*, ~~*4525*~~, Miqne VIb *4283* Miqne Vb *4282*, ~~*4284*~~	Megiddo K/4 =VIA: *3939, 3940, 3942, 3943, 3944, 3945, 3946* Qasile X: ~~*3853*~~, *3930, 3931,* ~~*3932*~~, *3933* Dor D2/9-10: *4531, 4532* Tel Hadar IV: *3795, 4291* Rehov D3: *3805,* ~~*3806*~~ Hammah [lower]: *4416*, 4417* Keisan 9b: ~~*3801*~~* Keisan 9a-b: *3802** Keisan 9a: *3796, 3803** Yoqneam XVII: *3777, 3778, 3779**		Hazor X: *3782*, 3783*, 3784, 3786* Megiddo H/5 [=IVB-VA]: ~~*3949*~~ Yoqneam XIV: *3780** Hammah [mid]: ~~*4411*~~, ~~*4412*~~, ~~*4413*~~, *4414, 4415, 4418, 4419, 4420, 4423, 4424, 4425* Dor D2/8b: *4556*	Safi IV: *4409,* ~~*4410*~~ Hammah [upper]: ~~*4422*~~ Hazor IX: *3785**	
Total: 2	**Total: 5(4)**	**Total: 9**	**Total: 27 (22)**	**Total: 4**	**Total: 18 (15)**	**Total: 4 (3)**	**Total: 6 (4)**
		Total: 51 (40)			**Total: 35 (24)**		
Total samples for model: 103 (78)							

The only samples not included in this model are 4288 from Tel Miqne (from a disturbed context) and 3987 from Beth Shemesh (unclear if late Iron I, Iron I|II, or Iron IIA). To avoid "infinite improbability" and non-converging simulations, we had to remove the worst misfits at the outset. This included, in addition to the 2 Hazor Middle Bronze Age dates and the Tel Zayit Middle Ages one, also 4501 (super-low Megiddo VII) and the 2 highest Moza dates (from the locus in which Bronze Age fragments were found; both these dates are entirely in the 12th–11th century—much too high for Iron II, on any chronology).

https://doi.org/10.1017/S0033822200041886 Published online by Cambridge University Press

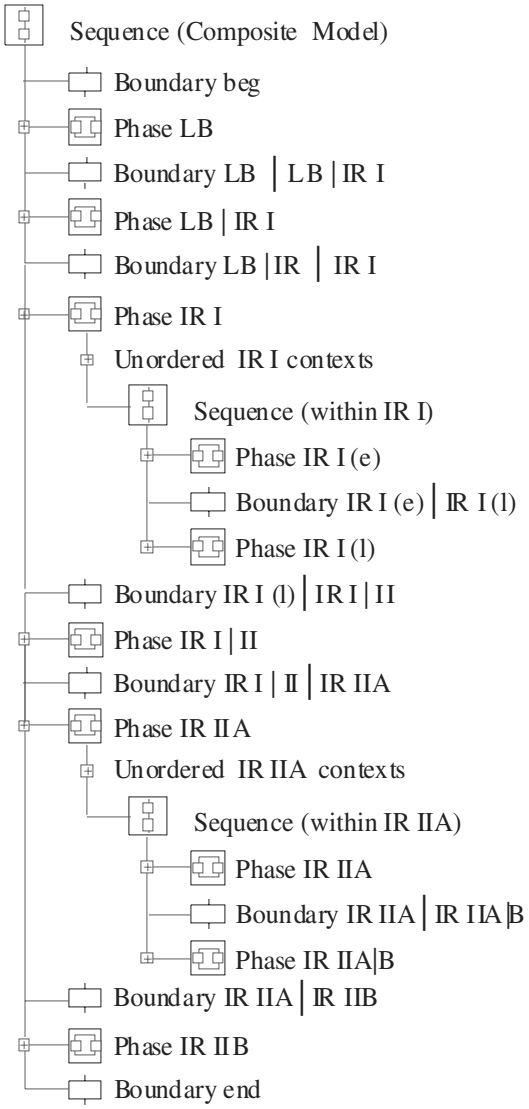

Figure 5 The composite model in OxCal notation

The composite model calculates a whole sequence of boundary distributions, but again, the ones of interest for the purpose of this study are between the (late) Iron I and the "transitional" Iron I|II horizon, and between the "transition" and the "classical" Iron IIA.

HANDLING MISFITS

We have already stressed the importance of systematic treatment of aberrant results. The high level of resolution attempted here, together with the fact that we refrained from a priori deleting measurements from the model unless we had external proof that they were erroneous, means that a certain amount of noise is inevitable. The replication protocol described above can often distinguish between errors generated in the laboratory—which would produce one or more outliers within a replicated set—and archaeological errors, either an out-of-context sample or a misattribution of the

https://doi.org/10.1017/S0033822200041886 Published online by Cambridge University Press

context. These would be manifest in internally consistent measurements that are out of order with the proposed sequence and would cause a poor fit between the data set and the model. To distinguish between the 2 types of errors, we call the first type "outliers" and the second "misfits" (Sharon et al. 2005:72–73, 77–78).

OxCal v 3.10 (Bronk Ramsey 2005) with atmospheric data from Reimer et al. (2004) provides a heuristic statistic for assessing the quality of the fit of the model, based on the overlap integral between the prior (unconstrained) measurement distribution and the posterior dating distribution (as constrained by the model). The rule of thumb is that an "agreement index" of 60% or more is a reasonable fit.

The strategy used here is as follows (see Figures 6–8): First, we present the results of the model with all misfitted results. This model usually shows very poor overall fit but has the merit of giving the best possible estimate of the dates of the transitions of interest—noise notwithstanding. Then, we start stepwise removal of misfits, beginning with the ones showing the lowest agreement index, until the overall agreement reaches 60%. We then present the "cleaned" model.

As it happens, the differences engendered by the stepwise removal of misfits, other than a gradual rise in the overall agreement index, were always very minor. Thus, the boundary distributions in both models, with and without the misfits, are always rather close.

RESULTS

A great number of OxCal runs were performed on the data set. We have 3 different models, and 3 different ways of combining (or not) replicated sets. Each of these 9 runs was repeated once on all types of samples, and once for short-lived samples only. Finally, we present 2 graphs of the results of each run, one before removal of misfits and one after "cleaning" misfitted results. This makes for 36 different assessments of the boundary-distributions between Iron I and Iron II in the Levant—times two in models where we include the "transitional" category itself and calculate both its beginning and end boundary (Figures 6–8).

The many different runs, under various presuppositions, serve to assess the vulnerability of the results to changes engendered not by the data itself, but the way it may be statistically analyzed. In the best case scenario—the "focused" model with only short-lived samples—we reach a 91% agreement with the removal of 3 misfits (out of 40 samples). We could have stopped after only 2 removals, but since all 3 had rather low agreement indices (under 10%) it seemed prudent to remove all of them. The noisiest model, as expected, is the "composite" model including long-lived charcoal samples. After the removal of 29 misfits (out of 103), the overall agreement index reached 56%. Almost one-third of the observations are misfitted. This is a rather high proportion. However, most of these do not relate to the boundaries of interest at all (but are, for example, too old to be in the Iron I at all, or misfitted vis-à-vis the Iron IIA|B transition). Also, a rather high proportion of the wood-charcoal samples turned out, in retrospect, to be indeed too old for their context (11 out of 25 charcoal samples in this study).

Figures 6–8 summarize the modeling runs. Each model includes the boundary distributions between Iron I and Iron II. Those models that include "transitional Iron I|II" contexts as a separate phase have *two* superimposed distributions on them. Also indicated are (40-yr-wide) acceptance regions for the alternative hypotheses regarding the Iron I|II transition: 1015–975 BCE for the High Chronology and 925–885 BCE for the Low to hyper Low. These are based on the differing historical backgrounds currently offered for the archaeological transition: Davidic conquests (dated by the Bible to the 1015–975 BCE region) by the High Chronology vs. the aftermath of the Shoshenq I campaign (about 925 BCE) by the Low Chronology.

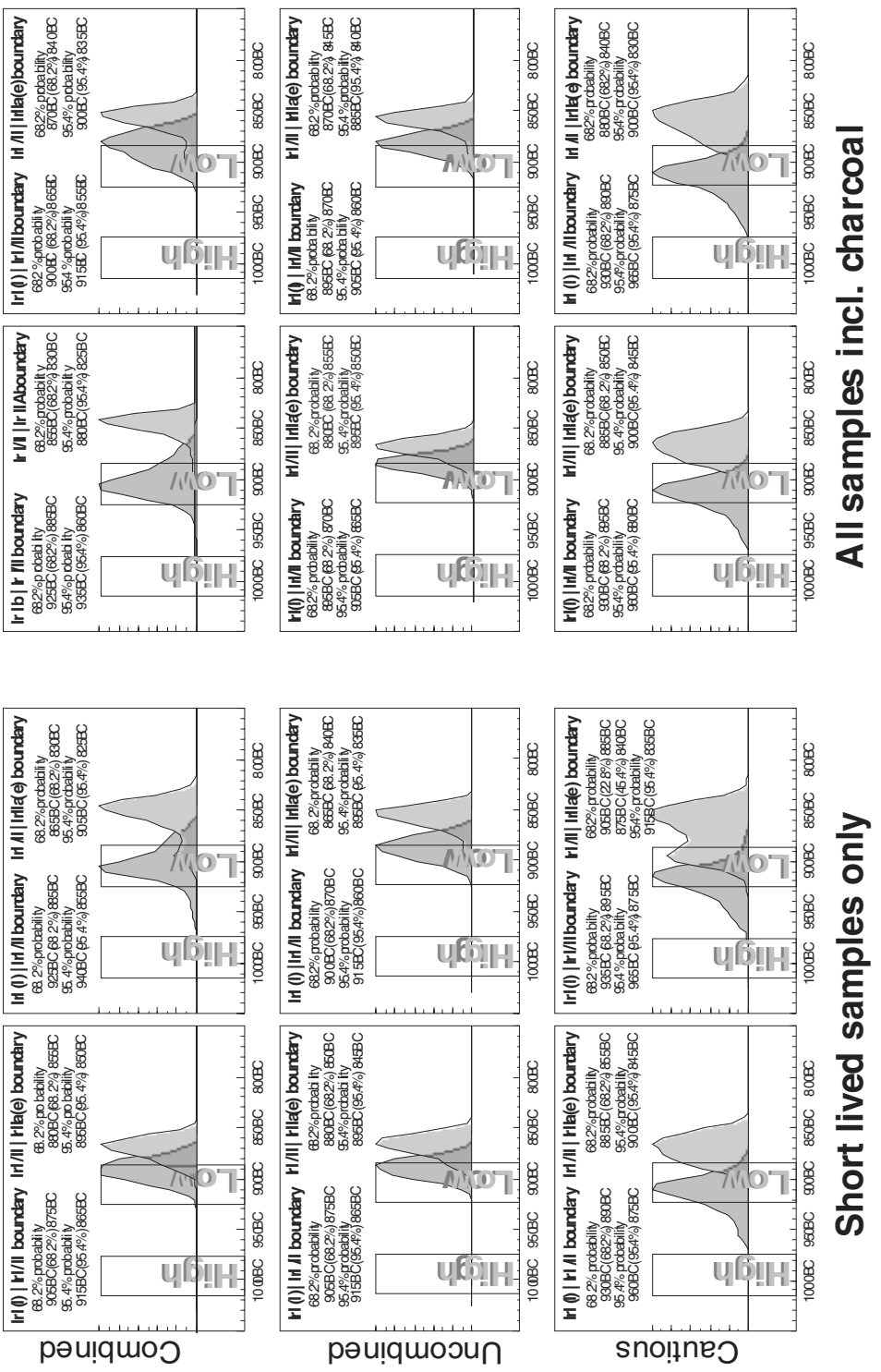

Figure 6 The focused model

https://doi.org/10.1017/S0033822200041886 Published online by Cambridge University Press

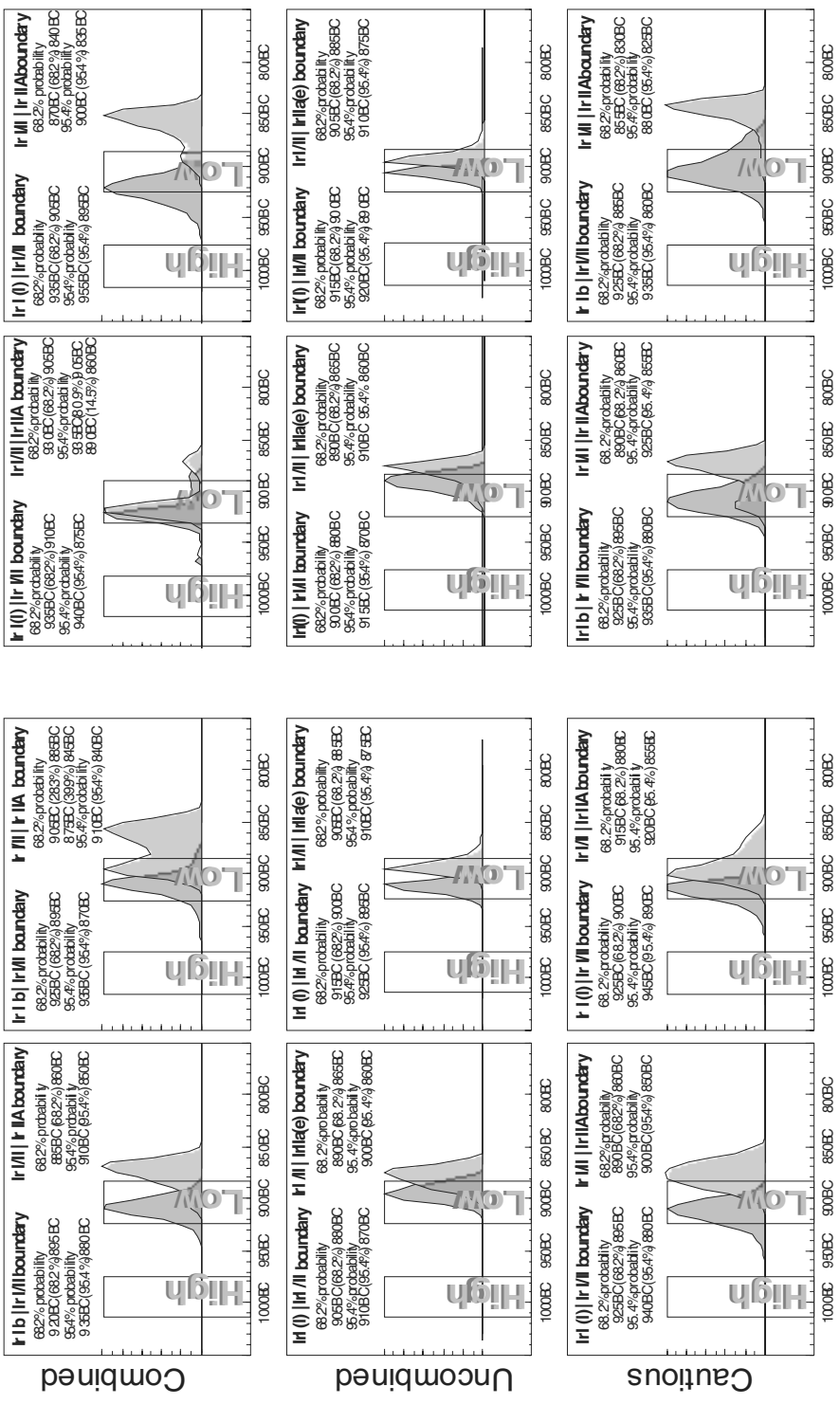

Figure 7 The composite model

https://doi.org/10.1017/S0033822200041886 Published online by Cambridge University Press

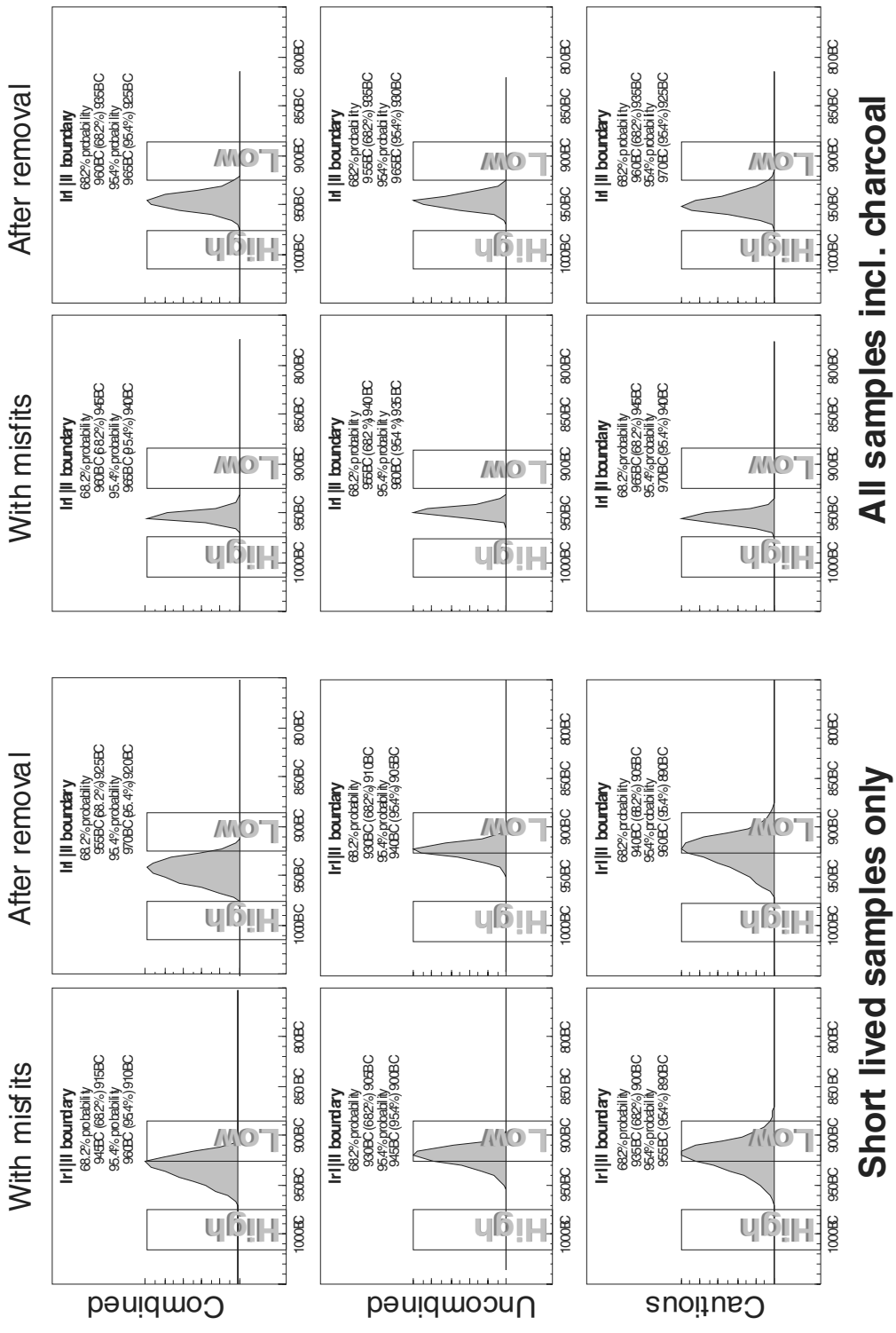

Figure 8 The coarse model

https://doi.org/10.1017/S0033822200041886 Published online by Cambridge University Press

Clearly, the choice of model and statistical treatment does affect the results, in the extreme case by as much as a century. The highest "transition" dates we got (the "coarse" model with charcoal) puts the transition at about 950, while the lowest possibilities (e.g. the "composite" model uncombined) put the Iron I (late) | Iron I|II boundary at about 890 and the Iron I|II | Iron IIA boundary at about 850 BCE. Typically, though, the models differ by a few decades at most, and this variability is over the 900–850 range. The highest "transition" date was reached by the "coarse" model, using a general division to Iron I contexts vs. Iron II and ignoring the critical transitional contexts, as well as including all the charcoal samples with the concomitant old-wood effect. But even in this extreme case, we get a transition in the mid-10th century, in between the 2 hypotheses. In all other model runs, the results hover around the Low Chronology range, with a transition between Iron I and Iron II around the turn of the 10th century. The "conventional"/"High" chronology (i.e. the "real" transition being at 980 BCE or earlier) is completely excluded by all models.

The results are also clearly dependent on the (relatively few) dates in the actual transitional (Iron I|II) range, as well as the highest dates in the early Iron IIA contexts and the lowest ones in the latest Iron I contexts. To investigate this dependence, we performed the following simple test. As the controversy now centers on the 10th century, we examined only those assays that produce distributions that are largely within the 10th century BCE. This was performed using only the 40 samples of the focused model (only short-lived samples from late Iron I, transitional Iron I|II, and Iron IIA contexts). Of these dates, the 10th century is occupied mainly by ones of late Iron I and "transitional" contexts (Table 6A), and this is true even when only the second half of that century is taken into account (Table 6B).

Table 6 A) Number of late Iron I, transitional Iron I|II, and Iron II combined dates (of short-lived samples only in the focused model) whose main distributions fall in the 10th century BCE. B) The same for the latter part of the 10th century. "Earlier than X" means that the 1-σ range is entirely above X, and the same for "later than Y."

(A)	Earlier than 980	10th century	Later than 920
Iron I (late)	8	10	3
Iron I|II	0	3	1
Iron IIA	0	2	13

(B)	Earlier than 940	Late 10th century	Later than 910
Iron I (late)	9	10	2
Iron I|II	0	3	1
Iron IIA	0	3	12

Will the inclusion of further results (e.g. already published results of other studies, or the second part of our own, or yet other dates that will undoubtedly be collected) critically tip the scale? It is hard to prophesy. For now, they point squarely within the Low Chronology. To see how much leeway there may be, we should also take a parting look at the calibration curve (Figure 1). The critical question is whether the small downwards wiggle at ~965 is in the Levantine Iron Age I, as we claim here, or in the Iron Age IIA range, as claimed by Mazar et al. Dates in the 2800–2850 BP range taken from Iron II contexts are needed to establish the High Chronology, while any additional dates in the 2790–2750 range from Iron I contexts will strengthen the Low one. If future dates prove similar to the ones hitherto obtained (by all projects), the transition dates will continue to hover within the second half of the 10th century BCE to the beginning of the 9th. For the United Monarchy debate, such dates

https://doi.org/10.1017/S0033822200041886 Published online by Cambridge University Press

will vindicate the assumptions of the Low Chronology, because starting Iron II at any point after about 975 BCE concedes that there is something flawed either in the biblical chronology, or its recount of events, or in the traditional link between material culture change and political history.

The results presented here were obtained using a much more comprehensive approach than previous works (Gilboa and Sharon 2001; Sharon 2001; Bruins et al. 2003; Mazar et al. 2005). The most important and, we hope, enduring result of this study is the large data set (Tables 7, 8), which, however interpreted, will serve as a basis for future chronologies of the Iron Age in the Levant and around the Mediterranean. We introduced here a replication protocol and rigorous methods of identifying and treating outliers. We used a regional approach and ceramic seriation to correlate the different contexts. Based on this, we tested many different models to assess the robustness of the data set and the models themselves. We did not try to date a single "historical event" but to introduce a series of transitions to help situate the temporal position and duration of phases in the archaeological record. Finally, we did not try to hide or explain away any of the misfits. All the dates—those that agree with the chronological framework proposed and those that contradict it—are herein presented.

Unlike historical dating, both ^{14}C and seriation are augmentative, progressive (in the sense that new and better data are continuously added), and probabilistic. Archaeologists relying on probabilistic tools will have to settle for probabilistic answers that indicate the highest likelihood for a given state-of-the-art. For the time being, our data set is definitely on the side of the Low Chronology and demonstrates that the Iron Age I|II transition occurred about the end of the 10th century BCE.

We have now entered the second stage of the Iron Age Dating Project. It involves the addition of many new dates to the database, mainly from recent excavations (but this time we use only clusters of short-lived samples), quality control on past and future samples using Raman spectroscopy (Alon et al. 2002), and the involvement of other laboratories. Inevitably, we believe, this is the only way to overcome the impasse regarding early Iron Age chronology in Israel.

ACKNOWLEDGMENTS

This research is being carried with the support of the Israel Science Foundation (grants Nos. 778/00; 141/04), the Kimmel Center of Archaeological Sciences at the Weizmann Institute of Science, the Research Authority at Hebrew University, the Research Authority at the University of Haifa, and the US National Science Foundation (Grant EAR01–15488). The first Tel Dor set of dates was produced in the 1990s by Israel Carmi, then director of the Rehovot laboratory. We are grateful for the full cooperation of all the excavators who contributed the samples for the project, from the following sites: Tell el-Akhwat (A Zertal), Aphek (M Kochavi and Y Gadot), Bethsaidah (R Arav), Beth Shemesh (S Bunimovitz and Z Lederman), Dor (E Stern), Tel Hadar (M Kochavi and E Yadin), Tell el-Hamma (J Cahill), Hazor (A Ben Tor), Hebron (E Eisenberg and the Israel Antiquities Authority), Tell Keisan (J-B Humbert), Megiddo (I Finkelstein, D Ussishkin, and B Halpern), Tel Miqne-Ekron (T Dothan and S Gitin), Moza (A De Groot, Z Greenhut, and the Israel Antiquities Authority), Tell Qasile (A Mazar), Tel Rehov (A Mazar), Kh Rosh Zayit (Z Gal and the Israel Antiquities Authority), Tell es-Safi-Gath (A Maeir), Shiloh (I Finkelstein), Sulem (Y Alexandre and the Israel Antiquities Authority), Yoqne'am (A Ben-Tor), and Tel Zayit (R Tappy). We wish to thank J van der Plicht of the Center for Isotope Research at Groningen for his cooperation in the intercomparison exercise regarding the Dor and other samples. Talia Goldman of the Hebrew University was of invaluable assistance in selecting the Tel Dor samples. We wish to specially thank Eugenia Mintz for the incredible and careful work done for the preparation of all the samples measured in this project.

Table 7 The Iron Age Dating Project database (January 2006). Sample numbers are identified by 4 digits. Individual measurements are identified by a prefix (indicating lab and measurement procedure) and sample number id. The 386 measurements of 105 samples are arranged by their relative chronological horizons. Weighted averages (W. AVG.) and combined error (C. σ) are calculated per sample. The standardized residual of each measurement from the weighted average is then calculated, and a χ^2 test is performed to test the significance of these deviations (columns χ^2, df, and α). Residuals significantly differing from the weighted average are highlighted. Entire lines highlighted mark outliers (as indicated by the χ^2 test), which were excluded from further analysis. In these cases, the W. AVG, C. σ, χ^2, df, and α in the highlighted row all designate the *initial* values of these statistics, while the same values in the non-highlighted rows give the values *after* exclusion of the outlier.

Site & context	Type	Sample	Analysis	^{14}C age (BP)	σ	W. AVG.	C. σ	Residual	χ^2	df	α	Relative date
Aphek X12 L3507	seeds	4510.3	Rehovot AMS	2949	40	2960	25	–0.2769	0.13	2	94%	LB
		4510.4	Rehovot AMS	2965	50			0.09848				
		4510.5	Rehovot AMS	2968	40			0.19811				
Tel Zayit L2009	olive pits	4274.3	Rehovot AMS	3000	40	3000	40	0	0	0	100%	LB
Megiddo K/6 (=VIIA?) 02/K/60	olive pits	4501.3	Rehovot AMS	2790	40	2775	25	0.37538	0.23	2	89%	LB|IR
		4501.4	Rehovot AMS	2764	50			–0.2197				
		4501.5	Rehovot AMS	2767	40			–0.1996				
Megiddo K/6 (=VIIA?) 02/K/60	olive pits	4499.3	Rehovot AMS	2880	40	2892	18	–0.293	1.43	4	84%	LB|IR
		4499.4	Rehovot AMS	2865	45			–0.5938				
		4499.5	Rehovot AMS	2925	40			0.83196				
		4499a	Tucson AMS	2907	40			0.38196				
		4499aa	Tucson AMS	2876	40			–0.393				
Megiddo K/6 (=VIIA?) 02/K/60	olive pits	4500.3	Rehovot AMS	2940	40	2933	18	0.17933	3.11	4	54%	LB|IR
		4500.4	Rehovot AMS	2906	37			–0.7251				
		4500.5	Rehovot AMS	2909	37			–0.644				
		4500a	Tucson AMS	3018	60			1.41955				
		4500aa	Tucson AMS	2947	40			0.35433				
Tel Miqne VIIb IVNW25102	seeds	4286.3	Rehovot AMS	2950	55	2907	28	0.78827	1.02	2	60%	LB|IR
		4286.4	Rehovot AMS	2900	40			–0.1661				
		4286.5	Rehovot AMS	2870	60			–0.6107				
Tell Keisan 13 8.7821	charcoal	3804.3	Rehovot AMS	2960	35	2989	17	–0.8226	1.22	4	87%	LB|IR
		3804.4	Rehovot AMS	2997	35			0.23456				

Table 7 The Iron Age Dating Project database (January 2006). Sample numbers are identified by 4 digits. Individual measurements are identified by a prefix (indicating lab and measurement procedure) and sample number id. The 386 measurements of 105 samples are arranged by their relative chronological horizons. Weighted averages (W. AVG.) and combined error (C. σ) are calculated per sample. The standardized residual of each measurement from the weighted average is then calculated, and a χ^2 test is performed to test the significance of these deviations (columns χ^2, df, and α). Residuals significantly differing from the weighted average are highlighted. Entire lines highlighted mark outliers (as indicated by the χ^2 test), which were excluded from further analysis. In these cases, the W. AVG, C. σ, χ^2, df, and α in the highlighted row all designate the *initial* values of these statistics, while the same values in the non-highlighted rows give the values *after* exclusion of the outlier. *(Continued)*

Site & context	Type	Sample	Analysis	^{14}C age (BP)	σ	W. AVG.	C. σ	Residual	χ^2	df	α	Relative date
		3804.5	Rehovot AMS	2996	35			0.20599				
		3804a	Tucson AMS	3022	50			0.66419				
		3804aa	Tucson AMS	2985	40			–0.0948				
El-Akhwat L3337	olive pits	4270.3	Rehovot AMS	2828	40	2815	23	0.33333	0.17	2	92%	Iron I
		4270.4	Rehovot AMS	2807	40			–0.1917				
		4270.5	Rehovot AMS	2809	40			–0.1417				
El-Akhwat L3357	olive pits	4271.3	Rehovot AMS	2858	40	2860	23	–0.05	0.07	2	97%	Iron I
		4271.4	Rehovot AMS	2854	40			–0.15				
		4271.5	Rehovot AMS	2868	40			0.2				
El-Akhwat L4323	olive pits	4272.3	Rehovot AMS	2822	40	2865	23	–1.075	4.67	2	10%	Iron I
		4272.4	Rehovot AMS	2838	40			–0.675				
		4272.5	Rehovot AMS	2935	40			1.75				
El-Akhwat L4332	olive pits	4273.3	Rehovot AMS	2847	40	2815	23	0.79167	1.42	2	49%	Iron I
		4273.4	Rehovot AMS	2819	40			0.09167				
		4273.5	Rehovot AMS	2780	40			–0.8833				
Hazor XII/XI L8037	charcoal	3700.3	Rehovot AMS	2975	35	2965	29	0.28188	0.24	1	62%	Iron I
		3700a	Tucson AMS	2945	50			–0.4027				
Hazor XII/XI L3690	charcoal	3701.3	Rehovot AMS	2940	30	2947	26	–0.2206	0.18	1	67%	Iron I
		3701a	Tucson AMS	2965	50			0.36765				
Hazor XII/XI L8254	olive pits	3702.1	Rehovot LSC	2935	25	2996	18	–2.4286	12.1	2	2%	Iron I
		3702.3	Rehovot AMS	3060	30			2.14286				
		3702a	Tucson AMS	3060	50			1.28571				

Table 7 The Iron Age Dating Project database (January 2006). Sample numbers are identified by 4 digits. Individual measurements are identified by a prefix (indicating lab and measurement procedure) and sample number id. The 386 measurements of 105 samples are arranged by their relative chronological horizons. Weighted averages (W. AVG.) and combined error (C. σ) are calculated per sample. The standardized residual of each measurement from the weighted average is then calculated, and a χ^2 test is performed to test the significance of these deviations (columns χ^2, df, and α). Residuals significantly differing from the weighted average are highlighted. Entire lines highlighted mark outliers (as indicated by the χ^2 test), which were excluded from further analysis. In these cases, the W. AVG, C. σ, χ^2, df, and α in the highlighted row all designate the *initial* values of these statistics, while the same values in the non-highlighted rows give the values *after* exclusion of the outlier. *(Continued)*

Site & context	Type	Sample	Analysis	^{14}C age (BP)	σ	W. AVG.	C. σ	Residual	χ^2	df	α	Relative date
Hazor XII/XI L8479	charcoal	3703.1	Rehovot LSC	3620	45	3616	29	0.0822	1.17	2	56%	Iron I
		3703.3	Rehovot AMS	3570	55			–0.8418				
		3703a	Tucson AMS	3650	50			0.67398				
Hazor XII/XI L8666	charcoal	3704.3	Rehovot AMS	3375	30	3374	27	0.03333	0.01	1	94%	Iron I
		3704a	Tucson AMS	3370	60			–0.0667	0.01			
Shiloh V L1301	raisins	3928.3	Rehovot AMS	2925	50	2897	23	0.55833	0.43	2	81%	Iron I
		3928.4	Rehovot AMS	2885	35			–0.3452				
		3928.5	Rehovot AMS	2895	40			–0.0521				
Shiloh V L335	seeds	3929.3	Rehovot AMS	2965	40	2959	28	0.1407	0.17	2	92%	Iron I
		3929.4	Rehovot AMS	2935	65			–0.375				
		3929.5	Rehovot AMS	2965	50			0.11256				
Tel Hevron VII L338	charcoal	4147.1	Rehovot LSC	3095	50	2989	29	2.11018	10.3	3	2%	Iron I
		4147.3	Rehovot AMS	3013	56			0.4198				
		4147.4	Rehovot AMS	2917	65			–1.1152				
		4147.5	Rehovot AMS	2852	65			–2.1152				
Tel Hevron VII L357	charcoal	4148.1	Rehovot LSC	3010	40	2984	18	0.66061	5.79	4	22%	Iron I
		4148.3	Rehovot AMS	3010	35			0.75498				
		4148.4	Rehovot AMS	2910	55			–1.3377				
		4148.5	Rehovot AMS	3025	40			1.03561				
		4148.6	Rehovot AMS	2935	35			–1.3879				
Tel Rehov D4 L1836	olive pits	3809.4	Rehovot AMS	2830	34	2878	15	–1.4134	5.22	5	39%	Iron I
		3809.5	Rehovot AMS	2861	35			–0.4873				
		3809a	Tucson AMS	2889	35			0.31266				

Table 7 The Iron Age Dating Project database (January 2006). Sample numbers are identified by 4 digits. Individual measurements are identified by a prefix (indicating lab and measurement procedure) and sample number id. The 386 measurements of 105 samples are arranged by their relative chronological horizons. Weighted averages (W. AVG.) and combined error (C. σ) are calculated per sample. The standardized residual of each measurement from the weighted average is then calculated, and a χ^2 test is performed to test the significance of these deviations (columns χ^2, df, and α). Residuals significantly differing from the weighted average are highlighted. Entire lines highlighted mark outliers (as indicated by the χ^2 test), which were excluded from further analysis. In these cases, the W. AVG, C. σ, χ^2, df, and α in the highlighted row all designate the *initial* values of these statistics, while the same values in the non-highlighted rows give the values *after* exclusion of the outlier. *(Continued)*

Site & context	Type	Sample	Analysis	^{14}C age (BP)	σ	W. AVG.	C. σ	Residual	χ^2	df	α	Relative date
		3809aa	Tucson AMS	2952	45			1.64318				
		GrA18825	Groningen AMS	2870	50			–0.1611				
		GrN261221	Groningen GPS	2890	30			0.3981				
Tel Miqne Vb (or IV??) IVNW27070	olive pits	4282.3	Rehovot AMS	2895	55	2876	20	0.34803	1.64	4	80%	Iron I
		4282.4	Rehovot AMS	2835	40			–1.0215				
		4282.5	Rehovot AMS	2900	50			0.48283				
		4282a	Tucson AMS	2872	40			–0.0965				
		4282aa	Tucson AMS	2895	40			0.47854				
Beth Shemesh 6 814	olive pits	3934.3	Rehovot AMS	2830	50	2855	29	–0.5	3.02	2	22%	Iron I (e)
		3934.4	Rehovot AMS	2925	50			1.4				
		3934.5	Rehovot AMS	2810	50			–0.9				
Beth Shemesh 5 160	olive pits	3935.3	Rehovot AMS	2830	53	2786	33	0.83068	1.18	2	55%	Iron I (e)
		3935.4	Rehovot AMS	2750	55			–0.6541				
		3935.5	Rehovot AMS	2770	65			–0.2458				
Beth Shemesh 5 393	olive pits	3936.3	Rehovot AMS	2810	50	2835	32	–0.4936	0.42	2	81%	Iron I (e)
		3936.4	Rehovot AMS	2850	55			0.27851				
		3936.5	Rehovot AMS	2855	65			0.31258				
Tel Dor D2/13 L19731	olive pits	4528.3	Rehovot AMS	2883	47	2909	24	–0.5632	0.56	2	76%	Iron I (e)
		4528.4	Rehovot AMS	2910	39			0.01353				
		4528.5	Rehovot AMS	2930	42			0.48875				
Tel Dor D2/12 L19707	olive pits	4522.3	Rehovot AMS	2868	50	2857	25	0.22944	0.08	2	96%	Iron I (e)
		4522.4	Rehovot AMS	2855	38			–0.0402				
		4522.5	Rehovot AMS	2850	43			–0.1518				

Table 7 The Iron Age Dating Project database (January 2006). Sample numbers are identified by 4 digits. Individual measurements are identified by a prefix (indicating lab and measurement procedure) and sample number id. The 386 measurements of 105 samples are arranged by their relative chronological horizons. Weighted averages (W. AVG.) and combined error (C. σ) are calculated per sample. The standardized residual of each measurement from the weighted average is then calculated, and a χ^2 test is performed to test the significance of these deviations (columns χ^2, df, and α). Residuals significantly differing from the weighted average are highlighted. Entire lines highlighted mark outliers (as indicated by the χ^2 test), which were excluded from further analysis. In these cases, the W. AVG, C. σ, χ^2, df, and α in the highlighted row all designate the *initial* values of these statistics, while the same values in the non-highlighted rows give the values *after* exclusion of the outlier. *(Continued)*

Site & context	Type	Sample	Analysis	^{14}C age (BP)	σ	W. AVG.	C. σ	Residual	χ^2	df	α	Relative date
Tel Dor D2/12 L19713	olive pits	4525.3	Rehovot AMS	2857	38	2847	22	0.2676	1.21	2	54%	Iron I (e)
		4525.4	Rehovot AMS	2869	38			0.58339				
		4525.5	Rehovot AMS	2811	40			–0.8958				
Tel Miqne VIB IVNW24062	olive pits	4283.3	Rehovot AMS	2915	45	2918	26	–0.0741	1.59	2	45%	Iron I (e)
		4283.4	Rehovot AMS	2960	45			0.92593				
		4283.5	Rehovot AMS	2880	45			–0.8519				
Tel Miqne VB IVNW10028	seeds	4284.3	Rehovot AMS	2835	45	2833	32	0.05556	0.01	1	94%	Iron I (e)
		4284.4	Rehovot AMS	2830	45							
Megiddo K/4 (=VIA) 98/K/036	seeds	3939.3	Rehovot AMS	2910	45	2804	24	2.34956	8.65	2	1%	Iron I (l)
		3939.4	Rehovot AMS	2790	40			–0.3567				
		3939.5	Rehovot AMS	2735	40			–1.7317				
Megiddo K/4 (=VIA) 98/K/037	seeds	3940.3	Rehovot AMS	2760	40	2767	25	–0.1773	0.06	2	97%	Iron I (l)
		3940.4	Rehovot AMS	2770	40			0.07271				
		3940.5	Rehovot AMS	2775	55			0.14379				
Megiddo K/4 (=VIA) 98/K/043	olive pits	3942.3	Rehovot AMS	2845	37	2846	20	–0.0237	0.17	3	98%	Iron I (l)
		3942.4	Rehovot AMS	2832	43			–0.3227				
		3942.5	Rehovot AMS	2856	42			0.241				
		3942.6	Rehovot AMS	2849	36			0.08672				
Megiddo K/4 (=VIA) 98/K/031	seeds	3943.3	Rehovot AMS	3045	40	2917	23	3.20833	15.5	2	0%	Iron I (l)
		3943.4	Rehovot AMS	2860	40	2853	28	0.1875	0.07	1	79%	
		3943.5	Rehovot AMS	2845	40			–0.1875				

Table 7 The Iron Age Dating Project database (January 2006). Sample numbers are identified by 4 digits. Individual measurements are identified by a prefix (indicating lab and measurement procedure) and sample number id. The 386 measurements of 105 samples are arranged by their relative chronological horizons. Weighted averages (W. AVG.) and combined error (C. σ) are calculated per sample. The standardized residual of each measurement from the weighted average is then calculated, and a χ^2 test is performed to test the significance of these deviations (columns χ^2, df, and α). Residuals significantly differing from the weighted average are highlighted. Entire lines highlighted mark outliers (as indicated by the χ^2 test), which were excluded from further analysis. In these cases, the W. AVG, C. σ, χ^2, df, and α in the highlighted row all designate the *initial* values of these statistics, while the same values in the non-highlighted rows give the values *after* exclusion of the outlier. *(Continued)*

Site & context	Type	Sample	Analysis	^{14}C age (BP)	σ	W. AVG.	C. σ	Residual	χ^2	df	α	Relative date
Megiddo K/4 (=VIA) 98/K/32	seeds	3944.3	Rehovot AMS	2975	60	2920	25	0.9155	4.3	3	23%	Iron I (l)
		3944.4	Rehovot AMS	2980	50			1.19859				
		3944.5	Rehovot AMS	2905	60			–0.2512				
		3944a	Tucson AMS	2864	40			–1.4018				
Megiddo K/4 (=VIA) 00/K/008	seeds	3945a	Tucson AMS	2858	40	2882	30	–0.5959	0.8	1	37%	Iron I (l)
		3945aa	Tucson AMS	2912	45			0.67034				
Megiddo K/4 (=VIA) 00/K/034	seeds	3946a	Tucson AMS	2910	35	2907	26	0.07434	0.01	1	91%	Iron I (l)
		3946aa	Tucson AMS	2904	40			–0.085				
Qasile X C653	lathyrus	3853.3	Rehovot AMS	2680	35	2753	22	–2.0884	12.9	2	0%	Iron I (l)
		3853.4	Rehovot AMS	2747	35			–0.1741				
		3853-1	Tucson AMS	2884	45			2.909				
Qasile X L168	lathyrus	3931.1	Rehovot LSC	2853	20	2864	13	–0.559	7.51	7	38%	Iron I (l)
		3931.3	Rehovot AMS	2820	55			–0.8033				
		3931.4	Rehovot AMS	2930	56			1.17535				
		3931.5	Rehovot AMS	2936	41			1.7517				
		3931-1	Tucson AMS	2852	45			–0.2707				
		GrA25535	Groningen AMS	2864	40			–0.0045				
		GrA25710	Groningen AMS	2818	38			–1.2153				
		GrA25768	Groningen AMS	2897	44			0.7459				
Qasile X L168	lathyrus	3932.3	Rehovot AMS	2745	50	2752	18	–0.1437	16.6	5	1%	Iron I (l)
		3932.4	Rehovot AMS	2765	75			0.17084				
		3932.5	Rehovot AMS	2685	50			–1.3437				
		3932.6	Rehovot AMS	2650	40			–2.5547				

Table 7 The Iron Age Dating Project database (January 2006). Sample numbers are identified by 4 digits. Individual measurements are identified by a prefix (indicating lab and measurement procedure) and sample number id. The 386 measurements of 105 samples are arranged by their relative chronological horizons. Weighted averages (W. AVG.) and combined error (C. σ) are calculated per sample. The standardized residual of each measurement from the weighted average is then calculated, and a χ^2 test is performed to test the significance of these deviations (columns χ^2, df, and α). Residuals significantly differing from the weighted average are highlighted. Entire lines highlighted mark outliers (as indicated by the χ^2 test), which were excluded from further analysis. In these cases, the W. AVG, C. σ, χ^2, df, and α in the highlighted row all designate the *initial* values of these statistics, while the same values in the non-highlighted rows give the values *after* exclusion of the outlier. *(Continued)*

Site & context	Type	Sample	Analysis	^{14}C age (BP)	σ	W. AVG.	C. σ	Residual	χ^2	df	α	Relative date
		3932a	Tucson AMS	2780	35			0.79467				
		3932aa	Tucson AMS	2862	40			2.74533				
Qasile X L134	seeds	3933a	Tucson AMS	2885	40	2882	28	0.0875	0.02	1	90%	Iron I (l)
		3933aa	Tucson AMS	2878	40			–0.0875				
Tel Dor D2/9-10 L19094	olive pits	4532.3	Rehovot AMS	2788	38	2783	22	0.13508	0.14	2	93%	Iron I (l)
		4532.4	Rehovot AMS	2771	39			–0.3043				
		4532.5	Rehovot AMS	2789	38			0.1614				
Tel Dor D2/9-10 L19098	olive pits	4531.3	Rehovot AMS	2756	38	2803	16	–1.2274	4.16	5	53%	Iron I (l)
		4531.4	Rehovot AMS	2808	38			0.14098				
		4531.5	Rehovot AMS	2849	38			1.21992				
		GrA25543	Groningen AMS	2769	40			–0.8411				
		GrA25712	Groningen AMS	2807	38			0.11466				
		GrA25772	Groningen AMS	2832	45			0.65238				
Tel Hadar IV L334	seeds	3795.3	Rehovot AMS	2791	52	2791	52	0	0	0	100%	Iron I (l)
Tel Hadar IV L334	seeds	4291.3	Rehovot AMS	2800	50	2853	13	–1.0573	16.1	7	2%	Iron I (l)
		4291.4	Rehovot AMS	2745	45			–2.397				
		4291.5	Rehovot AMS	2780	50			–1.4573				
		4291-3.1a	Rehovot LSC	2856	30			0.10451				
		4291-3.1b	Rehovot LSC	2852	30			–0.0288				
		4291-3.2	Rehovot AMS	2815	60			–0.6311				
		4291-5.1	Rehovot LSC	2901	30			2.03244				
		4291-4.1	Rehovot LSC	2924	35			1.60451				

Table 7 The Iron Age Dating Project database (January 2006). Sample numbers are identified by 4 digits. Individual measurements are identified by a prefix (indicating lab and measurement procedure) and sample number id. The 386 measurements of 105 samples are arranged by their relative chronological horizons. Weighted averages (W. AVG.) and combined error (C. σ) are calculated per sample. The standardized residual of each measurement from the weighted average is then calculated, and a χ^2 test is performed to test the significance of these deviations (columns χ^2, df, and α). Residuals significantly differing from the weighted average are highlighted. Entire lines highlighted mark outliers (as indicated by the χ^2 test), which were excluded from further analysis. In these cases, the W. AVG, C. σ, χ^2, df, and α in the highlighted row all designate the *initial* values of these statistics, while the same values in the non-highlighted rows give the values *after* exclusion of the outlier. *(Continued)*

Site & context	Type	Sample	Analysis	^{14}C age (BP)	σ	W. AVG.	C. σ	Residual	χ^2	df	α	Relative date
Tel Rehov D3 L2862	olive pits	3805.3	Rehovot AMS	2774	35	2803	19	–0.8351	1	3	80%	Iron I (l)
		3805.4	Rehovot AMS	2811	34			0.2286				
		3805.5	Rehovot AMS	2816	35			0.36493				
		GrA16757	Groningen AMS	2820	50			0.33545				
Tel Rehov D3 L1823	olive pits	3806.3	Rehovot AMS	2728	35	2754	24	–0.7497	1.09	1	30%	Iron I (l)
		3806.5	Rehovot AMS	2779	34			0.72827				
Tell el Hammah lower L384	charcoal	4416.3	Rehovot AMS	2801	40	2779	23	0.55833	0.54	2	76%	Iron I (l)
		4416.4	Rehovot AMS	2760	40			–0.4667				
		4416.5	Rehovot AMS	2775	40			–0.0917				
Tell el Hammah lower L384	semolina	4417.3	Rehovot AMS	2780	40	2790	23	–0.25	0.38	2	83%	Iron I (l)
		4417.4	Rehovot AMS	2810	40			0.5				
		4417.5	Rehovot AMS	2780	40			–0.25				
Tell Keisan 9a L502/5288	charcoal	3803.1	Rehovot LSC	2893	35	2868	15	0.71093	13.4	7	6%	Iron I (l)
		3803.3	Rehovot AMS	2817	50			–1.0224				
		3803.4	Rehovot AMS	2940	50			1.43765				
		3803.6	Rehovot AMS	2870	45			0.04183				
		3803.7	Rehovot AMS	2800	40			–1.7029				
		3803.8	Rehovot AMS	2800	40			–1.7029				
		3803a	Tucson AMS	2938	35			1.99664				
		3803aa	Tucson AMS	2862	65			–0.0941				
		3803.5	Rehovot AMS	2997	35	2888	14	3.10754	24.9	8	0%	
Tell Keisan 9a L610	seeds	3796.3	Rehovot AMS	2870	40	2855	29	0.38605	0.71	2	70%	Iron I (l)
		3796.4	Rehovot AMS	2875	70			2.29203				
		3796.5	Rehovot AMS	2820	50			–0.6912				

Table 7 The Iron Age Dating Project database (January 2006). Sample numbers are identified by 4 digits. Individual measurements are identified by a prefix (indicating lab and measurement procedure) and sample number id. The 386 measurements of 105 samples are arranged by their relative chronological horizons. Weighted averages (W. AVG.) and combined error (C. σ) are calculated per sample. The standardized residual of each measurement from the weighted average is then calculated, and a χ^2 test is performed to test the significance of these deviations (columns χ^2, df, and α). Residuals significantly differing from the weighted average are highlighted. Entire lines highlighted mark outliers (as indicated by the χ^2 test), which were excluded from further analysis. In these cases, the W. AVG, C. σ, χ^2, df, and α in the highlighted row all designate the *initial* values of these statistics, while the same values in the non-highlighted rows give the values *after* exclusion of the outlier. *(Continued)*

Site & context	Type	Sample	Analysis	^{14}C age (BP)	σ	W. AVG.	C. σ	Residual	χ^2	df	α	Relative date
Tell Keisan 9a-b L502/6085	charcoal	3802.1	Rehovot LSC	2870	35	2853	22	0.48178	1.52	3	68%	Iron I (l)
		3802.3	Rehovot AMS	2820	50			–0.6628				
		3802.4	Rehovot AMS	2820	50			–0.6628				
		3802.5	Rehovot AMS	2885	50			0.63725				
Tell Keisan 9b L514	charcoal	3801.1	Rehovot LSC	2935	35	2786	23	4.25045	33.2	3	0%	Iron I (l)
		3801.3	Rehovot AMS	2640	50	2674	30	–0.6711	1.41	2	49%	
		3801.4	Rehovot AMS	2720	50			0.92887				
		3801.5	Rehovot AMS	2655	60			–0.3093				
Yoqneam XVII(a) L3035	charcoal	3779.1	Rehovot LSC	2926	30	2875	21	1.68713	6.53	3	9%	Iron I (l)
		3779.3	Rehovot AMS	2815	45			–1.3419				
		3779.4	Rehovot AMS	2870	60			–0.0898				
		3779.5	Rehovot AMS	2800	55			–1.3707				
Yoqneam XVII(b?) L3041	olive pits	3777.1	Rehovot LSC	2866	15	2866	14	0.00182	2.22	3	53%	Iron I (l)
		3777.3	Rehovot AMS	2830	60			–0.5995				
		3777.4	Rehovot AMS	2910	45			0.97838				
		3777.5	Rehovot AMS	2790	80			–0.9497				
Yoqneam XVII(b?) L3047	olive pits	3778.1	Rehovot LSC	2776	15	2816	11	–2.6489	27.8	8	0%	Iron I (l)
		3778.3	Rehovot AMS	2780	45			–0.7941				
		3778/4	Rehovot AMS	2865	45			1.09479				
		3778.5	Rehovot AMS	2800	45			–0.3496				
		3778a	Tucson AMS	2780	45			–0.7941				
		3778aa	Tucson AMS	2855	40			0.98164				
		GrA25534	Groningen AMS	2925	38			2.87541				
		GrA25708	Groningen AMS	2897	38			2.13857				
		GrA25767	Groningen AMS	2929	54			2.09751				

Table 7 The Iron Age Dating Project database (January 2006). Sample numbers are identified by 4 digits. Individual measurements are identified by a prefix (indicating lab and measurement procedure) and sample number id. The 386 measurements of 105 samples are arranged by their relative chronological horizons. Weighted averages (W. AVG.) and combined error (C. σ) are calculated per sample. The standardized residual of each measurement from the weighted average is then calculated, and a χ^2 test is performed to test the significance of these deviations (columns χ^2, df, and α). Residuals significantly differing from the weighted average are highlighted. Entire lines highlighted mark outliers (as indicated by the χ^2 test), which were excluded from further analysis. In these cases, the W. AVG, C. σ, χ^2, df, and α in the highlighted row all designate the *initial* values of these statistics, while the same values in the non-highlighted rows give the values *after* exclusion of the outlier. *(Continued)*

Site & context	Type	Sample	Analysis	^{14}C age (BP)	σ	W. AVG.	C. σ	Residual	χ^2	df	α	Relative date
Tel Miqne IV/ pre I? IVNE(?)9022	olive pits	4288.3	Rehovot AMS	2615	40	2602	23	0.31667	2.8	2	25%	Iron I? /II?
		4288.4	Rehovot AMS	2550	40			–1.3083				
		4288.5	Rehovot AMS	2642	40			0.99167				
Beth Shemesh early 3?/4?? L876	charcoal	3987.1	Rehovot LSC	2880	35	2881	19	–0.0385	3.18	3	37%	Iron I (l)?/IIA?
		3987.3	Rehovot AMS	2844	34			–1.0985				
		3987.4	Rehovot AMS	2889	35			0.21861				
		3987.5	Rehovot AMS	2952	51			1.38532				
Tel Dor D2/8c L17333	olive pits	4540.3	Rehovot AMS	2724	49	2757	18	–0.6812	1.2	5	94%	Iron I|II
		4540.4	Rehovot AMS	2772	43			0.34008				
		4540.5	Rehovot AMS	2756	39			–0.0353				
		GrA25544	Groningen AMS	2741	38			–0.431				
		GrA25714	Groningen AMS	2776	39			0.47752				
		GrA25787	Groningen AMS	2792	76			0.45557				
Tel Dor D2/8c L17336	olive pits	4541.3	Rehovot AMS	2796	38	2764	22	0.85088	1.99	2	37%	Iron I|II
		4541.4	Rehovot AMS	2773	38			0.24561				
		4541.5	Rehovot AMS	2722	38			–1.0965				
Tel Dor D2/8c L17337	olive pits	4542.3	Rehovot AMS	2801	38	2779	24	0.58939	0.67	2	71%	Iron I|II
		4542.4	Rehovot AMS	2757	38			–0.5685				
		4542.5	Rehovot AMS	2777	54			–0.0297				
Aphek X8 L4015	seeds	4511.3	Rehovot AMS	2685	35	2667	20	0.52381	1.24	2	54%	Iron I|II
		4511.4	Rehovot AMS	2680	35			0.38095				
		4511.5	Rehovot AMS	2635	35			–0.9048				

Table 7 The Iron Age Dating Project database (January 2006). Sample numbers are identified by 4 digits. Individual measurements are identified by a prefix (indicating lab and measurement procedure) and sample number id. The 386 measurements of 105 samples are arranged by their relative chronological horizons. Weighted averages (W. AVG.) and combined error (C. σ) are calculated per sample. The standardized residual of each measurement from the weighted average is then calculated, and a χ^2 test is performed to test the significance of these deviations (columns χ^2, df, and α). Residuals significantly differing from the weighted average are highlighted. Entire lines highlighted mark outliers (as indicated by the χ^2 test), which were excluded from further analysis. In these cases, the W. AVG, C. σ, χ^2, df, and α in the highlighted row all designate the *initial* values of these statistics, while the same values in the non-highlighted rows give the values *after* exclusion of the outlier. *(Continued)*

Site & context	Type	Sample	Analysis	^{14}C age (BP)	σ	W. AVG.	C. σ	Residual	χ^2	df	α	Relative date
Bethsaida Str. 6 B#16426	seeds	4281.1a	Rehovot LSC	2820	35	2815	17	0.15622	3.69	4	45%	Iron IIA?
		4281.1b	Rehovot LSC	2866	35			1.47051				
		4281.3	Rehovot AMS	2775	50			–0.7906				
		4281.4	Rehovot AMS	2800	40			–0.3633				
		4281.5	Rehovot AMS	2780	40			–0.8633				
Tel Rehov D2? L1802	olive pits	3807.1a	Rehovot LSC	2760	30	2784	11	–0.8005	6.8	5	24%	Iron IIA(?)
		3807.1b	Rehovot LSC	2783	35			–0.029				
		3807.3	Rehovot AMS	2763	35			–0.6005				
		3807.4	Rehovot AMS	2716	35			–1.9433				
		3807.5	Rehovot AMS	2793	36			0.24955				
		GrN26112	Groningen GPS	2805	15			1.39892				
Rosh Zayit IIA L23	seeds	3797.3	Rehovot AMS	2597	63	2709	15	–1.7831	9.09	8	33%	Iron IIA
		3797.4	Rehovot AMS	2766	65			0.87177				
		3797.5	Rehovot AMS	2695	44			–0.3258				
		3797.6	Rehovot AMS	2660	40			–1.2334				
		3797.7	Rehovot AMS	2762	40			1.31662				
		3797.8	Rehovot AMS	2750	40			1.01662				
		3797-1.1	Rehovot AMS	2670	50			–0.7867				
		3797-1.2	Rehovot AMS	2715	45			0.12589				
		3797-1.3	Rehovot AMS	2725	45			0.34811				
Rosh Zayit IIA L53	seeds	3798.1	Rehovot LSC	2745	30	2733	15	0.39181	3.47	5	63%	Iron IIA
		3798.3	Rehovot AMS	2760	40			0.66886				
		3798.4	Rehovot AMS	2755	40			0.54386				
		3798.3	Rehovot AMS	2750	40			0.41886				
		3798a	Tucson AMS	2687	35			–1.3213				
		3798aa	Tucson AMS	2693	50			–0.8049				

Table 7 The Iron Age Dating Project database (January 2006). Sample numbers are identified by 4 digits. Individual measurements are identified by a prefix (indicating lab and measurement procedure) and sample number id. The 386 measurements of 105 samples are arranged by their relative chronological horizons. Weighted averages (W. AVG.) and combined error (C. σ) are calculated per sample. The standardized residual of each measurement from the weighted average is then calculated, and a χ^2 test is performed to test the significance of these deviations (columns χ^2, df, and α). Residuals significantly differing from the weighted average are highlighted. Entire lines highlighted mark outliers (as indicated by the χ^2 test), which were excluded from further analysis. In these cases, the W. AVG, C. σ, χ^2, df, and α in the highlighted row all designate the *initial* values of these statistics, while the same values in the non-highlighted rows give the values *after* exclusion of the outlier. *(Continued)*

Site & context	Type	Sample	Analysis	^{14}C age (BP)	σ	W. AVG.	C. σ	Residual	χ^2	df	α	Relative date
Rosh Zayit IIA L52	seeds	3799.1	Rehovot LSC	2745	30	2722	19	0.76735	1.88	3	60%	Iron IIA
		3799.3	Reh AMS (avg)	2730	40			0.20051				
		3799a	Tucson AMS	2683	35			–1.1137				
		3799aa	Tucson AMS	2728	70			0.08601				
Sulem L108	charcoal	3989.3	Rehovot AMS	2837	40	2838	28	–0.025	0	1	97%	Iron IIA
		3989.4	Rehovot AMS	2839	40			0.025				
Sulem L108	charcoal	3990.3	Rehovot AMS	2915	40	2865	24	1.25288	2.8	2	25%	Iron IIA
		3990.4	Rehovot AMS	2821	40			–1.0971				
		3990.5	Rehovot AMS	2857	45			–0.1752				
Sulem L111	charcoal	3991.3	Rehovot AMS	2642	35	2669	21	–0.7832	6.85	2	3%	Iron IIA
		3991.4	Rehovot AMS	2629	35			–1.1546				
		3991.5	Rehovot AMS	2758	40			2.214689				
Tel Rehov E1b L2618	olive pits	3808.3	Rehovot AMS	2693	35	2680	16	0.37555	0.62	4	96%	Iron IIA
		3808.4	Rehovot AMS	2671	35			–0.253				
		3808.5	Rehovot AMS	2669	35			–0.3102				
		3808a	Tucson AMS	2671	35			–0.253				
		3808aa	Tucson AMS	2700	40			0.50361				
Hazor Xa L8034	charcoal	3782.3	Rehovot AMS	2680	55	2645	31	0.64311	3.83	2	15%	Iron IIA (e)
		3782.4	Rehovot AMS	2570	50			–1.4926				
		3782.5	Rehovot AMS	2710	60			1.08952				
Hazor Xa L8034	charcoal	3783.3	Rehovot AMS	2822	40	2741	18	2.02778	11.2	4	2%	Iron IIA (e)
		3783.4	Rehovot AMS	2680	50			–1.2178				
		3783.5	Rehovot AMS	2796	40			1.37778				
		3783a	Tucson AMS	2731	40			–0.2472				
		3783aa	Tucson AMS	2674	35			–1.9111				

Table 7 The Iron Age Dating Project database (January 2006). Sample numbers are identified by 4 digits. Individual measurements are identified by a prefix (indicating lab and measurement procedure) and sample number id. The 386 measurements of 105 samples are arranged by their relative chronological horizons. Weighted averages (W. AVG.) and combined error (C. σ) are calculated per sample. The standardized residual of each measurement from the weighted average is then calculated, and a χ^2 test is performed to test the significance of these deviations (columns χ^2, df, and α). Residuals significantly differing from the weighted average are highlighted. Entire lines highlighted mark outliers (as indicated by the χ^2 test), which were excluded from further analysis. In these cases, the W. AVG, C. σ, χ^2, df, and α in the highlighted row all designate the *initial* values of these statistics, while the same values in the non-highlighted rows give the values *after* exclusion of the outlier. *(Continued)*

Site & context	Type	Sample	Analysis	^{14}C age (BP)	σ	W. AVG.	C. σ	Residual	χ^2	df	α	Relative date
Hazor Xa L8579	olive pits	3784.3	Rehovot AMS	2620	80	2632	27	–0.1475	2.61	3	46%	Iron IIA (e)
		3784.4	Rehovot AMS	2570	50			–1.2359				
		3784.5	Rehovot AMS	2680	50			0.96406				
		3784.6	Rehovot AMS	2650	50			0.36406				
Hazor Xb L8595	olive pits	3786.4	Rehovot AMS	2450	50	2610	22	–3.2052	15.1	4	0%	Iron IIA (e)
		3786.3	Rehovot AMS	2615	80	2650	25	–0.4409	2.29	3	51%	
		3786.5	Rehovot AMS	2695	50			0.89449				
		3786a	Tucson AMS	2576	66			–1.1254				
		3786aa	Tucson AMS	2656	35			0.16356				
Megiddo H/5 (IVB-VA) (3949.3)	seeds	3949.3	Rehovot AMS	2820	50	2817	23	0.06575	3.99	3	26%	Iron IIA (e)
		3949.4	Rehovot AMS	2900	50			1.66575				
		3949a	Tucson AMS	2788	40			–0.7178				
		3949aa	Tucson AMS	2775	50			–0.8342				
Tel Dor D2/8b L17230	olive pits	4556.3	Rehovot AMS	2765	43	2750	23	0.34286	1.63	2	44%	Iron IIA (e)
		4556.4	Rehovot AMS	2777	38			0.70377				
		4556.5	Rehovot AMS	2712	38			–1.0068				
Tell el Hammah mid L117	seeds	4411.1a	Rehovot LSC	2830	35	2815	29	0.42282	0.54	1	46%	Iron IIA (e)
		4411.1b	Rehovot LSC	2785	50			–0.604				
Tell el Hammah mid L119	seeds	4412.3	Rehovot AMS	2663	40	2609	21	1.35593	3.41	2	18%	Iron IIA (e)
		4412.4	Rehovot AMS	2611	35			0.06392				
		4412.5	Rehovot AMS	2565	35			–1.2504				
Tell el Hammah mid L466	seeds	4413.3	Rehovot AMS	2576	40	2587	23	–0.275	0.2	2	90%	Iron IIA (e)
		4413.4	Rehovot AMS	2601	40			0.35				
		4413.5	Rehovot AMS	2584	40			–0.075				

Table 7 The Iron Age Dating Project database (January 2006). Sample numbers are identified by 4 digits. Individual measurements are identified by a prefix (indicating lab and measurement procedure) and sample number id. The 386 measurements of 105 samples are arranged by their relative chronological horizons. Weighted averages (W. AVG.) and combined error (C. σ) are calculated per sample. The standardized residual of each measurement from the weighted average is then calculated, and a χ^2 test is performed to test the significance of these deviations (columns χ^2, df, and α). Residuals significantly differing from the weighted average are highlighted. Entire lines highlighted mark outliers (as indicated by the χ^2 test), which were excluded from further analysis. In these cases, the W. AVG, C. σ, χ^2, df, and α in the highlighted row all designate the *initial* values of these statistics, while the same values in the non-highlighted rows give the values *after* exclusion of the outlier. *(Continued)*

Site & context	Type	Sample	Analysis	^{14}C age (BP)	σ	W. AVG.	C. σ	Residual	χ^2	df	α	Relative date
Tell el Hammah mid L117	seeds	4414.3	Rehovot AMS	2652	40	2634	23	0.45	0.59	2	75%	Iron IIA (e)
		4414.4	Rehovot AMS	2640	40			0.15				
		4414.5	Rehovot AMS	2610	40			–0.6				
Tell el Hammah mid L117	seeds	4415.3	Rehovot AMS	2648	40	2636	23	0.3	0.8	2	67%	Iron IIA (e)
		4415.4	Rehovot AMS	2607	40			–0.725				
		4415.5	Rehovot AMS	2653	40			0.425				
Tell el Hammah mid L117	seeds	4418.3	Rehovot AMS	2700	40	2722	24	–0.547	1.82	2	40%	Iron IIA (e)
		4418.4	Rehovot AMS	2765	40			1.07799				
		4418.5	Rehovot AMS	2695	45			–0.5973				
Tell el Hammah mid L119	seeds	4419.3	Rehovot AMS	2715	40	2728	28	–0.3125	0.2	1	66%	Iron IIA (e)
		4419.4	Rehovot AMS	2740	40			0.3125				
Tell el Hammah mid L119	seeds	4420.3	Rehovot AMS	2725	40	2675	23	1.25	2.84	2	24%	Iron IIA (e)
		4420.4	Rehovot AMS	2630	40			–1.125				
		4420.5	Rehovot AMS	2670	40			–0.125				
Tell el Hammah mid L117	semolina	4423.3	Rehovot AMS	2710	35	2688	25	0.64286	0.83	1	36%	Iron IIA (e)
		4423.4	Rehovot AMS	2665	35			–0.6429				
Tell el Hammah mid L119	semolina	4424.3	Rehovot AMS	2700	35	2687	20	0.38095	0.26	2	88%	Iron IIA (e)
		4424.4	Rehovot AMS	2685	35			–0.0476				
		4424.5	Rehovot AMS	2675	35			–0.3333				
Tell el Hammah mid L117	semolina	4425.3	Rehovot AMS	2740	35	2701	22	1.11104	2.01	2	37%	Iron IIA (e)
		4425.4	Rehovot AMS	2680	45			–0.4692				
		4425.5	Rehovot AMS	2675	35			–0.7461				

Table 7 The Iron Age Dating Project database (January 2006). Sample numbers are identified by 4 digits. Individual measurements are identified by a prefix (indicating lab and measurement procedure) and sample number id. The 386 measurements of 105 samples are arranged by their relative chronological horizons. Weighted averages (W. AVG.) and combined error (C. σ) are calculated per sample. The standardized residual of each measurement from the weighted average is then calculated, and a χ^2 test is performed to test the significance of these deviations (columns χ^2, df, and α). Residuals significantly differing from the weighted average are highlighted. Entire lines highlighted mark outliers (as indicated by the χ^2 test), which were excluded from further analysis. In these cases, the W. AVG, C. σ, χ^2, df, and α in the highlighted row all designate the *initial* values of these statistics, while the same values in the non-highlighted rows give the values *after* exclusion of the outlier. *(Continued)*

Site & context	Type	Sample	Analysis	^{14}C age (BP)	σ	W. AVG.	C. σ	Residual	χ^2	df	α	Relative date
Yoqneam XIVb L1734	charcoal	3780.1	Rehovot LSC	2735	30	2711	14	0.79681	5.71	6	46%	Iron IIA (e)
		3780.1a	Rehovot LSC	2716	25			0.19617				
		3780.3	Rehovot AMS	2635	45			–1.691				
		3780.4	Rehovot AMS	2657	55			–0.9836				
		3780.5	Rehovot AMS	2665	70			–0.6585				
		3780	Tucson AMS	2740	35			0.82583				
		3780	Tucson AMS	2725	45			0.30898				
Hazor IXa L8087	olive pits	3785.4	Rehovot AMS	2675	50	2692	21	–0.3461	0.36	4	99%	Iron IIA|B
		3785.5	Rehovot AMS	2710	50			0.35392				
		3785.6	Rehovot AMS	2680	50			–0.2461				
		3785a	Tucson AMS	2693	35			0.01988				
		3785aa	Tucson AMS	2705	55			0.23083				
Moza L2043	charcoal	4583.3	Rehovot AMS	2857	40	2855	25	0.06209	0.27	2	87%	Iron IIA?
		4583.4	Rehovot AMS	2865	40			0.26209				
		4583.5	Rehovot AMS	2830	55			–0.4458				
Moza L2043	charcoal	4584.3	Rehovot AMS	2908	40	2898	23	0.24167	0.18	2	91%	Iron IIA?
		4584.4	Rehovot AMS	2885	40			–0.3333				
		4584.5	Rehovot AMS	2902	40			0.09167				
Moza L2043	charcoal	4586.3	Rehovot AMS	2813	40	2816	23	–0.0833	0.01	2	99%	Iron IIA?
		4586.4	Rehovot AMS	2819	40			0.06667				
		4586.5	Rehovot AMS	2817	40			0.01667				
Moza L2043	charcoal	4587.3	Rehovot AMS	2873	40	2906	28	–0.8125	1.32	1	25%	Iron IIA?
		4587.4	Rehovot AMS	2938	40			0.8125				

Table 7 The Iron Age Dating Project database (January 2006). Sample numbers are identified by 4 digits. Individual measurements are identified by a prefix (indicating lab and measurement procedure) and sample number id. The 386 measurements of 105 samples are arranged by their relative chronological horizons. Weighted averages (W. AVG.) and combined error (C. σ) are calculated per sample. The standardized residual of each measurement from the weighted average is then calculated, and a χ^2 test is performed to test the significance of these deviations (columns χ^2, df, and α). Residuals significantly differing from the weighted average are highlighted. Entire lines highlighted mark outliers (as indicated by the χ^2 test), which were excluded from further analysis. In these cases, the W. AVG, C. σ, χ^2, df, and α in the highlighted row all designate the *initial* values of these statistics, while the same values in the non-highlighted rows give the values *after* exclusion of the outlier. *(Continued)*

Site & context	Type	Sample	Analysis	^{14}C age (BP)	σ	W. AVG.	C. σ	Residual	χ^2	df	α	Relative date
Tel es-Safi IV L22042	seeds	4409.3	Rehovot AMS	2630	45	2661	30	–0.6794	0.87	2	65%	Iron IIA|B
		4409.4	Rehovot AMS	2693	60			0.54043				
		4409.5	Rehovot AMS	2679	55			0.33502				
Tel es-Safi IV L22042	seeds	4410.3	Rehovot AMS	2748	60	2723	18	0.42126	3.62	5	61%	Iron IIA|B
		4410.4	Rehovot AMS	2671	45			–1.1494				
		4410.5	Rehovot AMS	2712	45			–0.2383				
		GrA25536	Groningen AMS	2700	42			–0.5411				
		GrA25711	Groningen AMS	2733	38			0.27041				
		GrA25770	Groningen AMS	2780	44			1.30172				
Tell el Hammah upper L205	seeds + sediment	4422.3	Rehovot AMS	2654	35	2588	20	1.88571	5.5	2	6%	Iron IIA|B
		4422.4	Rehovot AMS	2565	35			–0.6571				
		4422.5	Rehovot AMS	2545	35			–1.2286				
Tel Zayit I L1477	seeds + charcoal	4275-1.3	Rehovot AMS	2640	40	2623	16	0.41827	7.49	6	28%	Iron IIB
		4275-1.4	Rehovot AMS	2646	45			0.50513				
		4275-1.5	Rehovot AMS	2745	55			2.21329				
		4275-2.3	Rehovot AMS	2616	40			–0.1817				
		4275-3.3	Rehovot AMS	2573	40			–1.2567				
		4275-3.4	Rehovot AMS	2605	40			–0.4567				
		4275-3.5	Rehovot AMS	2600	40			–0.5817				
Tel Zayit I L1477	olive pits	4278.3	Rehovot AMS	1400	35	1415	20	–0.4286	2	2	37%	Iron IIB
		4278.4	Rehovot AMS	1390	35			–0.7143				
		4278.5	Rehovot AMS	1455	35			1.14286				
Tel Zayit I L1476	charcoal	4279.4	Rehovot AMS	2681	35	2682	25	–0.0286	0	1	97%	Iron IIB
		4279.5	Rehovot AMS	2683	35			0.02857				

Table 7 The Iron Age Dating Project database (January 2006). Sample numbers are identified by 4 digits. Individual measurements are identified by a prefix (indicating lab and measurement procedure) and sample number id. The 386 measurements of 105 samples are arranged by their relative chronological horizons. Weighted averages (W. AVG.) and combined error (C. σ) are calculated per sample. The standardized residual of each measurement from the weighted average is then calculated, and a χ^2 test is performed to test the significance of these deviations (columns χ^2, df, and α). Residuals significantly differing from the weighted average are highlighted. Entire lines highlighted mark outliers (as indicated by the χ^2 test), which were excluded from further analysis. In these cases, the W. AVG, C. σ, χ^2, df, and α in the highlighted row all designate the *initial* values of these statistics, while the same values in the non-highlighted rows give the values *after* exclusion of the outlier. *(Continued)*

Site & context	Type	Sample	Analysis	^{14}C age (BP)	σ	W. AVG.	C. σ	Residual	χ^2	df	α	Relative date
Tel Zayit I L1476	charcoal	4280.3	Rehovot AMS	2615	40	2634	28	–0.475	0.45	1	50%	Iron IIB
		4280.4	Rehovot AMS	2653	40			0.475				
Beth Shemesh 3 L297	olive pits	3937.1	Rehovot LSC	2500	35	2482	17	0.52527	4.11	3	25%	Iron IIB
		3937.3	Rehovot AMS	2524	36			1.17735				
		3937.4	Rehovot AMS	2427	35			–1.5604				
		3937.5	Rehovot AMS	2478	34			–0.1063				
Beth Shemesh 3 L488	olive pits	3938.3	Rehovot AMS	2390	65	2453	26	–0.9701	3.12	2	21%	Iron IIB
		3938.4	Rehovot AMS	2425	40			–0.7015				
		3938.5	Rehovot AMS	2505	40			1.29851				
# of samples: 105			**# of dates: 386** **# of excluded outliers: 4**						**308.56**	**278**	**10.04%**	

Table 8 Calibrated dates. Two dates are given per sample. The first uses the weighted average and combined error of the replicated set, after removal of outliers where necessary. The second uses the "cautious" error estimation procedure, using the *wider* of 2 estimates: 1) the combined date as above and 2) the unweighted average and standard deviation between replications. Dates were calibrated using the IntCal04 calibration curve (Reimer et al. 2004). Note that single ranges are quoted, i.e. the extreme edges of the highest-density regions, ignoring gaps that may exist within the region. For the relevant area on the calibration curve, such gaps rarely exceed a decade or so.

			Combined measures				Cautious estimation			
Site & stratum	Relative date	Type	μ	σ	68% range	95% range	μ	σ	68% range	95% range
Aphek X12 (4510)	LB	seeds	2960	25	1260–1120 BC	1290–1050 BC	2960	25	1260–1120 BC	1290–1050 BC
Tel Zayit (4274)	LB	seeds	3000	40	1370–1130 BC	1390–1120 BC	3000	40	1370–1130 BC	1390–1120 BC
Megiddo K/6 (VIIA?) (4501)	LB|Ir	olive pits	2775	25	980–850 BC	1000–840 BC	2775	25	980–850 BC	1000–840 BC
Megiddo K/6 (VIIA?) (4499)	LB|Ir	olive pits	2892	18	1120–1040 BC	1130–1000 BC	2891	22	1120–1040 BC	1190–1000 BC
Megiddo K/6 (VIIA?) (4500)	LB|Ir	olive pits	2933	18	1210–1090 BC	1260–1050 BC	2944	40	1260–1050 BC	1300–1010 BC
Tel Miqne VIIb (4286)	LB|Ir	seeds	2907	28	1190–1030 BC	1210–1000 BC	2907	33	1190–1020 BC	1260–1000 BC
Tell Keisan 13 (3804)	LB|Ir	charcoal	2989	17	1270–1130 BC	1310–1120 BC	2992	20	1300–1130 BC	1320–1120 BC
El-Ahwat (4270)	Ir I	olive pits	2815	23	1000–925 BC	1030–900 BC	2815	23	1000–925 BC	1030–900 BC
El-Ahwat (4271)	Ir I	olive pits	2860	23	1110–970 BC	1120–930 BC	2860	23	1110–970 BC	1120–930 BC
El-Ahwat (4272)	Ir I	olive pits	2865	23	1120–990 BC	1130–940 BC	2865	50	1120–940 BC	1210–900 BC
El-Ahwat (4273)	Ir I	olive pits	2815	23	1000–925 BC	1030–900 BC	2815	27	1005–925 BC	1050–900 BC
Hazor XII/XI (3700)	Ir I	charcoal	2965	29	1260–1120 BC	1310–1050 BC	2965	29	1260–1120 BC	1310–1050 BC
Hazor XII/XI (3701)	Ir I	charcoal	2947	26	1260–1120 BC	1270–1050 BC	2947	26	1260–1120 BC	1270–1050 BC
Hazor XII/XI (3702)	Ir I	olive pits	2996	18	1295–1210 BC	1320–1120 BC	3018	59	1390–1130 BC	1420–1050 BC
Hazor XII/XI (3703)	Ir I	charcoal	3616	29	2025–1935 BC	2120–1890 BC	3613	33	2025–1930 BC	2120–1880 BC
Hazor XII/XI (3704)	Ir I	charcoal	3374	27	1730–1625 BC	1750–1600 BC	3374	27	1730–1625 BC	1750–1600 BC
Shiloh V (3927)	Ir I	seeds	2854	25	1060–940 BC	1120–930 BC	2854	25	1060–940 BC	1120–930 BC
Shiloh V (3928)	Ir I	raisins	2897	23	1125–1040 BC	1200–1000 BC	2897	23	1125–1040 BC	1200–1000 BC
Shiloh V (3929)	Ir I	fava beans	2959	28	1260–1120 BC	1290–1050 BC	2959	28	1260–1120 BC	1290–1050 BC
Tel Hevron VII (4147)	Ir I	charcoal	2989	34	1300–1130 BC	1380–1110 BC	2965	96	1370–1040 BC	1420–920 BC
Tel Hevron VII (4148)	Ir I	charcoal	2984	18	1270–1130 BC	1300–1120 BC	2978	46	1300–1120 BC	1380–1050 BC
Tel Rehov D4 (3809)	Ir I	olive pits	2878	15	1115–1010 BC	1120–1000 BC	2882	37	1130–1000 BC	1210–930 BC
Beth Shemesh 5 (3935)	Ir I(e)	olive pits	2786	33	1000–895 BC	1010–840 BC	2783	34	1000–895 BC	1010–830 BC
Beth Shemesh 5 (3936)	Ir I(e)	olive pits	2835	32	1040–920 BC	1120–900 BC	2835	32	1040–920 BC	1120–900 BC
Beth Shemesh 6 (3934)	Ir I(e)	olive pits	2855	29	1060–930 BC	1130–920 BC	2855	50	1120–930 BC	1210–900 BC
Tel Dor D2/12 (4522)	Ir I(e)	olive pits	2857	25	1060–940 BC	1120–930 BC	2857	25	1060–940 BC	1120–930 BC

Table 8 Calibrated dates. Two dates are given per sample. The first uses the weighted average and combined error of the replicated set, after removal of outliers where necessary. The second uses the "cautious" error estimation procedure, using the *wider* of 2 estimates: 1) the combined date as above and 2) the unweighted average and standard deviation between replications. Dates were calibrated using the IntCal04 calibration curve (Reimer et al. 2004). Note that single ranges are quoted, i.e. the extreme edges of the highest-density regions, ignoring gaps that may exist within the region. For the relevant area on the calibration curve, such gaps rarely exceed a decade or so. *(Continued)*

			Combined measures				Cautious estimation			
Site & stratum	Relative date	Type	μ	σ	68% range	95% range	μ	σ	68% range	95% range
Tel Dor D2/12 (4525)	Ir I(e)	olive pits	2847	22	1045–945 BC	1120–920 BC	2846	25	1050–940 BC	1120–920 BC
Tel Dor D2/13 (4528)	Ir I(e)	olive pits	2909	24	1190–1040 BC	1210–1010 BC	2909	24	1190–1040 BC	1210–1010 BC
Tel Miqne Vb (4284)	Ir I(e)	seeds	2832	32	1025–925 BC	1120–900 BC	2832	32	1025–925 BC	1120–900 BC
Tel Miqne VIb (4283)	Ir I(e)	olive pits	2918	26	1200–1050 BC	1220–1010 BC	2918	33	1200–1040 BC	1260–1010 BC
Megiddo K/4 (VIA) (3939)	Ir I(l)	seeds	2804	24	995–915 BC	1020–890 BC	2762	28	970–840 BC	1000–830 BC
Megiddo K/4 (VIA) (3940)	Ir I(l)	seeds	2767	25	970–840 BC	1000–830 BC	2767	25	970–840 BC	1000–830 BC
Megiddo K/4 (VIA) (3942)	Ir I(l)	olive seeds	2846	20	1045–945 BC	1090–920 BC	2846	20	1045–945 BC	1090–920 BC
Megiddo K/4 (VIA) (3943)	Ir I(l)	seeds	2852	28	1060–940 BC	1120–920 BC	2917	91	1270–1000 BC	1390–900 BC
Megiddo K/4 (VIA) (3944)	Ir I(l)	seeds	2920	25	1200–1050 BC	1250–1010 BC	2931	49	1260–1050 BC	1310–990 BC
Megiddo K/4 (VIA) (3945)	Ir I(l)	seeds	2882	30	1120–1010 BC	1200–940 BC	2882	30	1120–1010 BC	1200–940 BC
Megiddo K/4 (VIA) (3946)	Ir I(l)	seeds	2907	26	1190–1030 BC	1210–1000 BC	2907	26	1190–1030 BC	1210–1000 BC
Qasile X (3853)	Ir I(l)	seeds	2714	25	895–825 BC	910–810 BC	2770	85	1010–820 BC	1160–790 BC
Qasile X (3930)	Ir I(l)	seeds	2800	25	995–915 BC	1020–850 BC	2797	33	1000–910 BC	1040–840 BC
Qasile X (3931)	Ir I(l)	seeds	2864	13	1050–1000 BC	1120–970 BC	2871	43	1130–970 BC	1210–910 BC
Qasile X (3932)	Ir I(l)	seeds	2724	20	900–835 BC	910–820 BC	2748	68	980–820 BC	1060–790 BC
Qasile X (3933)	Ir I(l)	seeds	2882	28	1115–1010 BC	1200–940 BC	2882	28	1115–1010 BC	1200–940 BC
Tel Dor D2/9-10 (4531)	Ir I(l)	olive pits	2803	16	980–920 BC	1005–905 BC	2804	33	1000–915 BC	1050–840 BC
Tel Dor D2/9-10 (4532)	Ir I(l)	olive pits	2783	22	975–900 BC	1010–840 BC	2783	22	975–900 BC	1010–840 BC
Tel Hadar IV (3795)	Ir I(l)	seeds	2791	52	1010–850 BC	1090–820 BC	2791	52	1010–850 BC	1090–820 BC
Tel Hadar IV (4291)	Ir I(l)	seeds	2856	13	1050–995 BC	1120–930 BC	2841	57	1120–910 BC	1210–840 BC
Tel Rehov D3 (3805)	Ir I(l)	olive pits	2803	19	980–915 BC	1010–900 BC	2803	19	980–915 BC	1010–900 BC
Tel Rehov D3 (3806)	Ir I(l)	olive pits	2754	24	920–840 BC	980–820 BC	2754	26	920–840 BC	980–820 BC
Tell el Hammah lower (4416)	Ir I(l)	charcoal	2779	23	975–895 BC	1000–840 BC	2779	23	975–895 BC	1000–840 BC
Tell el Hammah lower (4417)	Ir I(l)	semolina	2790	23	975–905 BC	1010–850 BC	2790	23	975–905 BC	1010–850 BC
Tell Keisan 9a (3803)	Ir I(l)	charcoal	2868	15	1070–1000 BC	1120–970 BC	2880	65	1190–930 BC	1270–890 BC
Tell Keisan 9a (3796)	Ir I(l)	seeds	2855	29	1060–930 BC	1130–920 BC	2855	29	1060–930 BC	1130–920 BC
Tell Keisan 9a-b (3802)	Ir I(l)	charcoal	2853	22	1050–940 BC	1120–930 BC	2849	29	1050–930 BC	1120–920 BC

Table 8 Calibrated dates. Two dates are given per sample. The first uses the weighted average and combined error of the replicated set, after removal of outliers where necessary. The second uses the "cautious" error estimation procedure, using the *wider* of 2 estimates: 1) the combined date as above and 2) the unweighted average and standard deviation between replications. Dates were calibrated using the IntCal04 calibration curve (Reimer et al. 2004). Note that single ranges are quoted, i.e. the extreme edges of the highest-density regions, ignoring gaps that may exist within the region. For the relevant area on the calibration curve, such gaps rarely exceed a decade or so. *(Continued)*

			Combined measures				Cautious estimation			
Site & stratum	Relative date	Type	μ	σ	68% range	95% range	μ	σ	68% range	95% range
Tell Keisan 9b (3801)	Ir I(l)	charcoal	2674	30	890–800 BC	895–795 BC	2738	118	1050–790 BC	1300–500 BC
Yoqneam XVII(a) (3779)	Ir I(l)	charcoal	2875	21	1120–1000 BC	1130–970 BC	2853	50	1120–930 BC	1210–890 BC
Yoqneam XVII(b?) (3777)	Ir I(l)	olive pits	2866	14	1055–1000 BC	1120–970 BC	2849	44	1110–920 BC	1200–900 BC
Yoqneam XVII(b?) (3778)	Ir I(l)	olive pits	2857	15	1055–995 BC	1120–930 BC	2845	60	1120–920 BC	1210–840BC
Tel Miqne Vb (4282)	Ir I?	olive pits	2876	20	1120–1000 BC	1130–970 BC	2879	24	1120–1010 BC	1130–970 BC
Tel Miqne IVa?/b? (pre I?) (4288)	Ir I?/II?	olive pits	2602	23	805–780 BC	815–765 BC	2602	39	815–765 BC	840–590 BC
Tel Rehov D2? (3807)	Ir I?/II?	olive pits	2784	11	975–905 BC	1000–895 BC	2770	29	980–840 BC	1000–830 BC
Aphek X-8 (4511)	Ir I|II	seeds	2667	20	830–805 BC	895–795 BC	2667	22	830–800 BC	895–795 BC
Tel Dor D2/8c (4540)	Ir I|II	olive pits	2757	18	925–845 BC	980–830 BC	2760	23	930–840 BC	980–830 BC
Tel Dor D2/8c (4541)	Ir I|II	olive pits	2764	22	970–840 BC	980–830 BC	2764	31	970–840 BC	1000–830 BC
Tel Dor D2/8c (4542)	Ir I|II	olive pits	2779	24	975–895 BC	1000–840 BC	2779	24	975–895 BC	1000–840 BC
Rosh Zayit IIA (3797)	Ir IIa	seeds	2709	15	895–820 BC	900–815 BC	2704	52	900–810 BC	980–790 BC
Rosh Zayit IIA (3798)	Ir IIa	seeds	2733	15	900–840 BC	915–830 BC	2732	30	905–835 BC	930–810 BC
Rosh Zayit IIA (3799)	Ir IIa	seeds	2722	19	895–830 BC	910–820 BC	2722	23	895–830 BC	915–815 BC
Sulem (3989)	Ir IIa	charcoal	2838	28	1040–930 BC	1120–910 BC	2838	28	1040–930 BC	1120–910 BC
Sulem (3990)	Ir IIa	charcoal	2865	24	1120–990 BC	1130–930 BC	2864	39	1120–970 BC	1200–910 BC
Sulem (3991)	Ir IIa	charcoal	2669	21	830–800 BC	895–795 BC	2669	21	830–800 BC	895–795 BC
Tel Rehov E1b (3808)	Ir IIa	olive pits	2680	16	835–805 BC	895–800 BC	2680	16	835–805 BC	895–800 BC
Hazor Xa (3782)	Ir IIa(e)	charcoal	2741	18	905–840 BC	925–830 BC	2653	60	900–780 BC	980–590 BC
Hazor Xa (3783)	Ir IIa(e)	charcoal	2720	20	895–830 BC	910–815 BC	2720	49	905–815 BC	980–790 BC
Hazor Xa (3784)	Ir IIa(e)	olive pits	2632	27	815–790 BC	835–775 BC	2630	41	830–785 BC	900–760 BC
Hazor Xb (3786)	Ir IIa(e)	olive pits	2650	25	825–795 BC	890–790 BC	2598	84	850–540 BC	920–410 BC
Megiddo H/5 (IVB-VA) (3949)	Ir IIa(e)	seeds	2817	23	1005–930 BC	1040–900 BC	2821	49	1050–910 BC	1130–840 BC
Tel Dor D2/8b (4556)	Ir IIa(e)	olive pits	2750	23	920–840 BC	970–820 BC	2751	28	920–840 BC	980–820 BC
Tell el Hammah mid (4411)	Ir IIa(e)	seeds	2815	29	1005–925 BC	1050–890 BC	2815	29	1005–925 BC	1050–890 BC
Tell el Hammah mid (4420)	Ir IIa(e)	seeds	2675	23	835–800 BC	895–795 BC	2675	39	895–800 BC	910–790 BC

Table 8 Calibrated dates. Two dates are given per sample. The first uses the weighted average and combined error of the replicated set, after removal of outliers where necessary. The second uses the "cautious" error estimation procedure, using the *wider* of 2 estimates: 1) the combined date as above and 2) the unweighted average and standard deviation between replications. Dates were calibrated using the IntCal04 calibration curve (Reimer et al. 2004). Note that single ranges are quoted, i.e. the extreme edges of the highest-density regions, ignoring gaps that may exist within the region. For the relevant area on the calibration curve, such gaps rarely exceed a decade or so. *(Continued)*

			Combined measures				Cautious estimation			
Site & stratum	Relative date	Type	μ	σ	68% range	95% range	μ	σ	68% range	95% range
Tell el Hammah mid (4423)	Ir IIa(e)	semolina	2687	25	890–805 BC	895–800 BC	2687	25	890–805 BC	895–800 BC
Tell el Hammah mid (4424)	Ir IIa(e)	semolina	2687	20	890–805 BC	895–800 BC	2687	20	890–805 BC	895–800 BC
Tell el Hammah mid (4425)	Ir IIa(e)	semolina	2701	22	895–810 BC	900–805 BC	2698	30	895–810 BC	905–800 BC
Tell el Hammah mid (4412)	Ir IIa(e)	seeds	2609	21	805–785 BC	815–775 BC	2613	40	820–770 BC	900–590 BC
Tell el Hammah mid (4413)	Ir IIa(e)	seeds	2587	23	800–775 BC	810–670 BC	2587	23	800–775 BC	810–670 BC
Tell el Hammah mid (4414)	Ir IIa(e)	seeds	2634	23	815–795 BC	830–785 BC	2634	23	815–795 BC	830–785 BC
Tell el Hammah mid (4415)	Ir IIa(e)	seeds	2636	23	815–795 BC	830–785 BC	2636	23	815–795 BC	830–785 BC
Tell el Hammah mid (4418)	Ir IIa(e)	seeds	2722	24	895–830 BC	915–815 BC	2720	32	900–830 BC	930–800 BC
Tell el Hammah mid (4419)	Ir IIa(e)	seeds	2728	28	900–835 BC	930–810 BC	2728	28	900–835 BC	930–810 BC
Yoqneam XIVb (3780)	Ir IIa(e)	charcoal	2711	14	895–825 BC	900–815 BC	2696	39	895–805 BC	920–790 BC
Hazor IXa (3785)	Ir IIa(l)	olive pits	2692	21	890–805 BC	900–805 BC	2692	21	890–805 BC	900–805 BC
Bethsaida VI (4281)	Ir IIa?	seeds	2815	17	1000–930 BC	1010–910 BC	2808	33	1000–915 BC	1050–840 BC
Moza (4583)	Ir IIa?	charcoal	2855	25	1060–940 BC	1120–930 BC	2855	25	1060–940 BC	1120–930 BC
Moza (4584)	Ir IIa?	charcoal	2898	23	1125–1040 BC	1200–1000 BC	2898	23	1125–1040 BC	1200–1000 BC
Moza (4586)	Ir IIa?	charcoal	2816	23	1000–930 BC	1030–900 BC	2816	23	1000–930 BC	1030–900 BC
Moza (4587)	Ir IIa?	charcoal	2906	28	1160–1020 BC	1210–1000 BC	2906	32	1190–1020 BC	1260–1000 BC
Tel es-Safi IV (4409)	Ir IIa|b	seeds	2661	30	835–795 BC	900–790 BC	2661	30	835–795 BC	900–790 BC
Tel es-Safi IV (4410)	Ir IIa|b	seeds	2723	18	895–835 BC	910–820 BC	2724	35	905–830 BC	970–800 BC
Beth Shemesh IIIe?/IV?? (3987)	Ir IIa-b??	charcoal	2881	19	1115–1010 BC	1130–990 BC	2891	39	1130–1000 BC	1220–930 BC
Beth Shemesh III (3931)	Ir IIb	olive pits	2482	17	760–540 BC	770–520 BC	2482	36	760–530 BC	770–410 BC
Beth Shemesh III (3938)	Ir IIb	olive pits	2453	26	750–410 BC	760–410 BC	2440	48	740–410 BC	760–400 BC
Tel Zayit I (4275)	Ir IIb	olive pits	2623	16	810–795 BC	815–785 BC	2632	51	850–770 BC	920–590 BC
Tel Zayit I (4278)	Ir IIb	olive pits	1415	20	620–655 AD	600–660 AD	1415	29	610–655 AD	585–665 AD
Tel Zayit I (4279)	Ir IIb	charcoal	2682	25	890–805 BC	895–800 BC	2682	25	890–805 BC	895–800 BC
Tel Zayit I (4280)	Ir IIb	charcoal	2634	28	820–790 BC	840–775 BC	2634	28	820–790 BC	840–775 BC
Tell el Hammah upper (4422)	Ir IIb	seeds	2588	20	800–775 BC	810–760 BC	2588	47	820–590 BC	840–540 BC

REFERENCES

Alon D, Mintz G, Cohen I, Weiner S, Boaretto E. 2002. The use of Raman spectroscopy to monitor the removal of humic substances from charcoal: quality control for ^{14}C dating of charcoal. *Radiocarbon* 44(1): 1–11.

Anderson WP. 1990. The beginnings of Phoenician pottery: vessel shape, style, and ceramic technology in the early phases of the Phoenician Iron Age. *Bulletin of the American Schools of Oriental Research* 279:35–55.

Ben-Shlomo D, Shai I, Maeir AM. 2004. Late Philistine decorated ware ("Ashdod ware"): typology, chronology, and production centers. *Bulletin of the American Schools of Oriental Research* 335:1–35.

Ben-Tor A, Zarzecki-Peleg A. Forthcoming. The pottery of Iron IIA–IIB in the northern valleys and Upper Galilee. In: Gitin S, editor. *The Pottery of Ancient Israel and Its Neighbors from the Neolithic Through the Hellenistic Period*. Jerusalem: Israel Exploration Society.

Bevington PR, Robinson DK. 1992. *Data Reduction and Error Analysis for the Physical Sciences*. Boston: WCB/McGraw-Hill. 384 p.

Boaretto A, Jull AJT, Gilboa A, Sharon I. 2005. Dating the Iron Age I/II transition in Israel: first intercomparison results. *Radiocarbon* 47(1):39–55.

Botto M. 2004. Per una riconsiderazione della cronologia degli inizi della colonizzazione fenicia nel Mediterraneo centro-occidentale. *Mediterranea* 1:579–630. In Italian.

Bronk Ramsey C. 2001. Development of the radiocarbon calibration program OxCal. *Radiocarbon* 43(2A): 355–63.

Bronk Ramsey C. 2005. Improving the resolution of radiocarbon dating by statistical analysis. In: Levy T, Higham T, editors. *The Bible and Radiocarbon Dating: Archaeology, Text and Science*. London: Equinox. p 57–64.

Bruins HJ, van der Plicht J, Mazar A. 2003. ^{14}C dates from Tel Rehov: Iron-Age chronology, pharaohs and Hebrew kings. *Science* 300(5617):315–8.

Bruins HJ, van der Plicht J, Mazar A, Bronk Ramsey C, Manning SW. 2005. The Groningen radiocarbon series from Tel Rehov. In: Levy T, Higham T, editors. *The Bible and Radiocarbon Dating: Archaeology, Text and Science*. London: Equinox. p 271–93.

Coldstream JN. 1999. On chronology: the CG II mystery and its sequel. In: Iacovou M, Michaelides D, editors. *Cyprus: The Historicity of the Geometric Horizon.* Nicosia: University of Cyprus. p 109–18.

Coldstream JN. 2003. Some Aegean reactions to the chronological debate in the southern Levant. *Tel Aviv* 30:247–58.

D'Agata AL, Goren Y, Mommsen H, Schwedt A, Yasur-Landau A. 2005. Imported pottery of LH IIIC style from Israel. Style, provenance, and chronology. In: Laffineur R, Greco E, editors. *Aegeum 25, Emporia, Aegeans in the Central and Eastern Mediterranean*. Proceedings of the 10th international conference. Athens, Italian School of Archaeology, 14–18 April 2004, Université de Liege. p 371–9.

Dothan T. 1982. *The Philistines and Their Material Culture*. Jerusalem: Israel Exploration Society. 352 p.

Dothan T, Zukerman A. 2004. A preliminary study of the Myc IIIC:1 pottery assemblages from Tel Miqne-Ekron and Ashdod. *Bulletin of the American Schools of Oriental Research* 333:1–54.

Fantalkin A. 2001. Low Chronology and the Greek Protogeometric and Geometric pottery in the southern Levant. *Levant* 33:117–25.

Finkelstein I. 1996. The archaeology of the United Monarchy: an alternative view. *Levant* 27:177–87.

Finkelstein I. 2000. The Philistine settlements: when, how and how many. In: *The Philistines and Their World: A Reassessment*. University Museum Monograph 108, University Symposium Series 11. Philadelphia: University of Pennsylvania Museum. p 159–80.

Finkelstein I, Silberman NA. 2001. *The Bible Unearthed: Archaeology's New Vision of Ancient Israel and the Origin of Its Sacred Texts*. New York: Free Press. 400 p.

Finkelstein I, Silberman NA. 2006. *David and Solomon: In Search of the Bible's Sacred Kings and the Roots of the Western Tradition*. New York: Free Press. 352 p.

Finkelstein I, Piasetzky E. 2003. Wrong and right; high and low: ^{14}C dates from Tel Rehov and Iron Age chronology. *Tel Aviv* 30:283–95

Finkelstein I. 2005. A Low Chronology update: archaeology, history and the Bible. In: Levy T, Higham T, editors. *The Bible and Radiocarbon Dating: Archaeology, Text and Science.* London: Equinox. p 31–42.

Gilboa A. 1999a. The dynamics of Phoenician Bichrome pottery. *Bulletin of the American Schools of Oriental Research* 316:1–21.

Gilboa A. 1999b. The view from the east—Tel Dor and the earliest Cypro-Geometric exports to the Levant. In: Iacovou M, Michaelides D, editors. *Cyprus: The Historicity of the Geometric Horizon.* Nicosia: University of Cyprus.

Gilboa A, Sharon I. 2001. Early Iron Age radiometric dates from Tel Dor: preliminary implications for Phoenicia, and beyond. *Radiocarbon* 43(3):1343–51.

Gilboa A, Sharon I. 2003. An archaeological contribution to the early Iron Age chronological debate: alternative chronologies for Phoenicia and their effects on the Levant, Cyprus and Greece. *Bulletin of the American Schools of Oriental Research* 332:7–80.

Herzog Z, Singer-Avitz L. 2004. Redefining the centre: the emergence of state in Judah. *Tel Aviv* 31:209–44.

Holden C. 2003. Dates boost conventional wisdom about Solomon's splendor. *Science* 300(5617):229–31.

Iacovou M. 1999. *Excerpta Cypria geometrica*—materials for the history of Geometric Cyprus. In: Iacovou M, Michaelides D, editors. *Cyprus: The Historicity of the Geometric Horizon*. Nicosia: University of Cy-

prus. p 141–61.
James PJ, Thorpe IJ, Kokkinos N, Morkot R, Frankish J. 1992. *Centuries of Darkness: A Challenge to the Chronology of Old World Archaeology.* London: Jonathan Cape. 434 p.
Knoppers G, McConville JG, editors. 2000. *Reconsidering Israel and Judah: Recent Studies on the Deuteronomistic History.* Winona Lake: Eisenbrauns.
Kopcke G. 2002. 1000 B.C.E.? 900 B.C.E.? A Greek vase from Lake Galilee. In: Ehrenberg E, editor. *Leaving No Stones Unturned: Essays on the Ancient Near East and Egypt in Honor of Donald P. Hansen*. Winona Lake: Eisenbrauns. p 109–17.
Maeir AM. 2004. Philistine culture in transition: the transformation of Philistine culture as a process of "Creolization." Paper presented at the 4th International Congress on the Archaeology of the Ancient Near East. 1–7 April 2004, Berlin.
Manning SW, Weninger B, South AK, Kling B, Kuniholm, PI, Muhly JD, Hadjisavvas S, Sewell DA, Cadogan G. 2001. Absolute age range of the Late Cypriot IIC period on Cyprus. *Antiquity* 75(288):328–40.
Manning SW, Bronk Ramsey C, Kutschera W, Higham T, Kromer B, Steier P, Wild EM. 2006. Chronology for the Aegean Late Bronze Age 1700–1400 B.C. *Science* 312(5773):565–9.
Mazar A. 1990. *Archaeology of the Land of the Bible 10,000–586 B.C.E.* New York: Doubleday. 572 p.
Mazar A. 2004. Greek and Levantine Iron Age chronology: a rejoinder. *Israel Exploration Journal* 54:24–36.
Mazar A. 2005. The debate over the chronology of the Iron Age. In: Levy T, Higham T, editors. *The Bible and Radiocarbon Dating: Archaeology, Text and Science.* London: Equinox. p 15–30.
Mazar A, Bruins HJ, Panitz-Cohen N, van der Plicht J. 2005. Ladder of time at Tel Rehov: stratigraphy, archaeological context, pottery and radiocarbon dates. In: Levy T, Higham T, editors. *The Bible and Radiocarbon Dating: Archaeology, Text and Science*. London: Equinox. p 195–255.
Mederos Martín A. 2005. La cronología fenicia entre el Mediterráneo oriental y el occidental. *Anejos del Archivo Español de Arqueología* 33:305–46. In Spanish.
Nijboer AJ, van der Plicht J, Bietti Sestieri AM, de Santis A. 2001. A high chronology for the early Iron Age in central Italy. *Palaeohistoria* 41/42:163–76.
Reimer PJ, Baillie MGL, Bard E, Bayliss A, Beck JW, Bertrand C, Blackwell PG, Buck CE, Burr G, Cutler KB, Damon PE, Edwards RL, Fairbanks RG, Friedrich M, Guilderson TP, Hughen KA, Kromer B, McCormac FG, Manning S, Bronk Ramsey C, Reimer RW, Remmele S, Southon JR, Stuiver M, Talamo S, Taylor FW, van der Plicht J, Weyhenmeyer CE. 2004. IntCal04 terrestrial radiocarbon age calibration, 0–26 cal kyr BP. *Radiocarbon* 46(3):1029–58.
Renfrew C. 1992. Foreword. In: James PJ, Thorpe IJ, Kokkinos N, Morkot R, Frankish J, editors. *Centuries of Darkness.* London: Jonathan Cape. p xiii–xv.
Schreiber N. 2003. *The Cypro-Phoenician Pottery of the Iron Age*. Boston: Brill Academic Publishers. 384 p.
Scott EM. 2003. The Fourth International Radiocarbon Intercomparison (FIRI). *Radiocarbon* 45(2):35–150.
Sharon I. 2001. "Transition dating"—a heuristic mathematical approach to the collation of ^{14}C dates from stratified sequences. *Radiocarbon* 43(2A):345–54.
Sharon I, Gilboa A, Jull AJT, Boaretto E. 2005. The Early Iron Age Dating Project: introduction, methodology, progress report and an update on the Tel Dor radiometric dates. In: Levy T, Higham T, editors. *The Bible and Radiocarbon Dating: Archaeology, Text and Science* London: Equinox. p 65–92.
Sharon I, Gilboa A, Boaretto E. Forthcoming. ^{14}C and the early Iron Age of Israel – Where are we really at? A commentary on the Tel Rehov radiometric dates. In: Bietak M, editor. *The Synchronisation of Civilizations in the Eastern Mediterranean in the Second Millennium B.C.* Proceedings of the 2nd EuroConference of SCIEM 2000. 28 May–1 June 2003. Vienna: Österreichischen Akademie der Wissenschaften.
Stone BJ. 1995. The Philistines and acculturation: culture change and ethnic continuity in the Iron Age. *Bulletin of the American Schools of Oriental Research* 298:7–32.
Thompson TL. 1999. *The Mythic Past: Biblical Archaeology and the Myth of History.* New York: Basic Books. 436 p.
Torres Ortiz M. 1998. La cronología absoluta Europea y el inicio de la colonización fenicia en occidente: implicaciones cronológicas en chypre y el próximo oriente. *Complutum* 9:49–60. In Spanish.
Ussishkin D. 1985. Levels VII and VI at Tel Lachish and the end of the Late Bronze Age in Canaan. In: Tubb JN, editor. *Palestine in the Late Bronze Age. Papers in Honour of Olga Tufnell.* London: Institute of Archaeology. p 213–30.
Ward WA. 1992. The present status of Egyptian chronology. *Bulletin of the American Schools of Oriental Research* 288:53–66.
Ward WA, Joukowsky MS, Astrom P, editors. 1992. *The Crisis Years: The 12th century B.C. from Beyond the Danube to the Tigris.* Dubuque, Iowa: Kendall-Hunt. 224 p.
Yizhaq M, Mintz G, Cohen I, Khalaily H, Weiner S, Boaretto E. 2005. Quality controlled radiocarbon dating of bones and charcoal from the early Pre-Pottery Neolithic B (PPNB) of Motza (Israel). *Radiocarbon* 47(2):193–206.
Zarzecki-Peleg A. 2005. Trajectories of Iron Age settlement in north Israel and their implications for chronology. In: Levy T, Higham T, editors. *The Bible and Radiocarbon Dating: Archaeology, Text and Science.* London: Equinox. p 367–78.